Entropy-Based Reliability Analysis and Design in Slope Engineering

NAVJOT SINGH KANWAR

This Thesis is Submitted in the Partial Fulfillment of the Requirements for Degree of

Master Of Science

in

Civil Engineering

FACULTY OF ENGINEERING
LAKEHEAD UNIVERSITY

Thunder Bay, Ontario, Canada

FACULTY OF GRADUATE STUDIES

Submitted by

NAME OF STUDENT	Navjot Singh Kanwar
STUDENT NO.	0679101
DEGREE AWARDED	Master of Science
ACADEMIC UNIT	Civil Engineering
TITLE OF THESIS	Entropy Based Reliability Analysis and Design in Slope Engineering

This thesis has been prepared under my supervision and the candidate has complied with the Master's regulations.

Signature of supervisor:

Supervisors Name (Printed): Dr. Jian Deng

Abstract

Canada has a wide range of landslide types reflecting the diverse geomorphic and geologic environments in the nation's landscape. Many civil engineering projects are located on or near sloping ground, and thus are potentially subject to various kinds of slope instability, which often produces extensive property damage and occasionally loss of life. A typical example is the massive landslide occurred on the Nipigon River, north of the town of Nipigon, Ontario in the 1990, which involved an estimated 300,000 cubic meters of soil and extended almost 350m inshore with a maximum width of approximately 290m.

The traditional methods for slope stability investigation are reliant on deterministic approaches which involve an overall factor of safety to account for various uncertainties. It is found that critical geotechnical parameters such as shear strength parameters may be regarded as random variables respectively with a probability distribution rather than deterministic values or constants. In this research, an alternative approach of probabilistic reliability method is adopted in slope engineering, which allows for systematic analysis of uncertainties and for their inclusion in evaluating slope performance. The research focuses on entropy-based reliability analysis and design in slope engineering. The four sub topics are:

1. ***Introducing soil variables field testing by the vane shear test.***
2. ***Proposing an entropy-based distribution free modelling for soil variables.***
3. ***Developing a new reliability analysis method using entropy distributions.***
4. ***Application of approach in the Nipigon slope's analysis & design.***

Firstly, the research involves the application of the vane shear test on the

Nipigon slope to obtain values of undrained shear strength (S_u). Moreover, the research proposes an entropy-based distribution-free method for modeling of soil variables, using the combination of the maximum entropy formalism (MEF) and Akaike information criterion (AIC). The method is applied to generate the unbiased model for soil variables based on optimal-order moments from soil samples. The method can adjust the level of sophistication of the resulting probability as per the nature and quantity of data. Its application on soil data of the slope of the Nipigon River landslide area yields efficient results with the 3rd order being the optimal order representing the quantified information very precisely.

Further, the research introduces a new reliability method to conduct a reliability analysis of the Nipigon slope. The approach involves the modification of the first-order reliability method to consider the non-normal variables of the entropy distributions adequately, supported by GEO-Slope software model analysis and response surface method to develop an explicit performance function. The approach developed can incorporate the uncertainties effectively and proficiently. The results imply that the Nipigon slope is hazardous with a probability of failure value touching 40%. The comparison of the proposed modified FORM with the GEO-Slope based Monte Carlo simulation indicated similarities in the results, consequently certifying the efficiency of the proposed algorithm.

Ultimately, a reliability-based slope is designed for the Nipigon slope by implementing the proposed methodology. In the first case, pile reinforcement is applied to the failure slope to enhance the stability of the failure slope. However, the results display a spike in the reliability index, but the slope is found unstable. Therefore, the slope is redesigned by creating a homogeneous layer aided with pile reinforcement. The design reduces the probability of failure up to 10^{-6}, thereby making it stable.

Keywords: Slope stability; Akaike's information criterion; Maximum entropy principle; Performance function; Reliability based design; Vane shear field test.

Dedicated to my family

Acknowledgement

The fulfillment of this thesis was a vital endeavor which I would not have been able to achieve without the assistance of my family, friends, and professors. First and foremost, I would like to acknowledge my thesis supervisor Dr. Jian Deng, who with his extensive scientific expertise and analytical skills have equipped me with constant guidance during this thesis project, which has produced great achievement to me. Further, his technical and editorial remarks encouraged me to enhance the quality of my thesis.

I would like to provide a special thank to Dr. Wilson Wang and Dr. Liang Cui for their reviewing comments and helpful feedback. Additionally, I would like to present particular regard to Conrad Hagstrom, and Robert Timoon, lab technicians for their support and help in using lab resources.

I wish to bestow my appreciation to my parents, who love and support me through all my endeavors and are always to support and advice me whenever I need one. Finally, I want to show gratefulness to all my friends and student associates who contributed mutual assistance and help throughout the entire master's program.

Contents

List of Tables

List of Figures

Abbreviations

PDF	=	Probability Density Function
CDF	=	Cumulative Density Function
MEF	=	Maximum Entropy Formalism
AIC	=	Akaike's Information Criterion
FORM	=	First Order Reliability Method
MCS	=	Monte Carlo Simulation
RSM	=	Response Surface Method
RBD	=	Reliability Based Design
VST	=	Vane Shear Test
FOS	=	Factor of Safety
β	=	Reliability Index
γ	=	Unit Weight
p_f	=	Probability of Failure
C	=	Cohesion
$phi(\phi)$	=	Friction Angle
S_u	=	Undrained Shear Strength

Chapter 1

Introduction

1.1 Background and Recent Research

Slope failure is a downslope movement of soil or rock debris under the influence of natural or artificial disturbances which results in landslides, avalanches, flow of debris, rockfall, etc. (Nemcok, Pasek, & Rybar, 1972; Cruden, 1996; Hong, 2012). It is the most devastating and unpredictable naturally occurring hazard, second only to an earthquake (Survey, 2000). Slope failures are catastrophic due mostly to sufficient energy generated by the effect of debris movement (Hong, 2012). A typical example is the Haiyuan earthquake that triggered the Loess landslide, which resulted in nearly 100,000 fatalities (Close & McCormick, 1992). According to United Nations report in 2014, natural disasters have resulted in 2 trillion USD economic losses, and have affected more than 4 billion people all over the world (Kellet, 2014). Therefore, assessment and development of defensive techniques for these hazards is the priority of engineers and researchers in the present era.

The unshirkable responsibility of a civil engineer is to develop efficient systems that are reliable for society by analyzing risk and reducing failure. Engineers must forecast and prevent catastrophes in the system that can result from natural or accidental hazards. The methods needed to evaluate, prevent and alleviate risks associated with failure of a system due to geo-

hazards should be rationalized, innovative, and made efficient in order to secure the safety of the system and of society as whole.

Traditionally, the deterministic geotechnical design is adopted which emphasizes on taking partial or system factor of safety based on sound verdict and experience of an engineer. System safety relies upon a single safety factor in a deterministic approach. Hence, conventional methods lack in considering uncertainties explicitly associated with geotechnical structures, as the lower value of a safety factor can result in unsafe design, and a high level of a safety factor can be extremely expensive. Achieving precise safety system standards is a paramount goal. Therefore, a more rationalized approach is needed to incorporate variabilities and uncertainties of the system to explicitly design a safe and reliable structure.

Consequently, an alternative approach of probabilistic analysis is considered more reliable to analyze structure stability. With respect to slope stability analysis, probabilistic slope stability analysis allows a comprehensive technique to evaluate the probability of slope failure by incorporating slope-specific variabilities and uncertainties. The design enhanced by probabilistic analysis is also more economical, and less likely to collapse in case of geohazard event.

1.2 Problem Formulation

Present geotechnical engineering designs are based on the concept of deterministic methods, considering a single factor of safety design based on the experience and judgment of the engineer. The deterministic approach framework lacks in incorporating uncertainties associated with the structure in an explicit form, and lacks in evaluating the probability of structure failure rather than relying on a single factor of safety. In the case of geotechnical slopes failures, foremost, it is necessary to quantify the available data

of geotechnical variables explicitly, and secondly, precisely predict the failure probability of the slope in a particular time frame. Accordingly, this research study focuses on proposing a distribution free probabilistic modeling of soil variables, and new modified First Order Reliability Method approach of reliability to analyze slope stability in a more effective framework.

This thesis includes considerations for different aspects associated with slope stability, which include more rationalized ways to quantify information about random variables obtained through field soil tests by using a distribution-free approach. Adopting probabilistic methods that can incorporate uncertainties and variabilities associated with variables of soil, obtained explicitly through field tests to determine the probability of slope failure. This study will derive a correlation between different layers of slope in view of a specific case study on the Nipigon River landslide.

1.3 Research Objective

The principal objective of the thesis is to carry out slope stability analysis on the soil variables obtained from the Nipigon River landslide site using field soil tests. Firstly, the variables obtained by field tests considered as random variables are to be quantified using distribution-free maximum entropy formalism (MEF), as well as Akaiki's information criterion (AIC) advanced probabilistic analysis. Secondly, the reliability analysis will be carried out by entropy-based modified first-order reliability method (FORM). Thirdly, a reliability analysis of the Nipigon River landslide slope reinforced with piles will be performed using GEO-Slope-based direct Monte Carlo simulation software. To accomplish these goals, various topics on geostatistics, probability, reliability, and uncertainties have been studied extensively.

1.4 Thesis Outline

The structure of the thesis has been shown in Figure 1.1.

Chapter 1 familiarizes with some introductory topics and problems involved in slope stability.

Chapter 2 presents a review of previous research and studies on different methods of slope stability analysis.

Chapter 3 familiarizes the developed entropy-based probabilistic method for soil variables quantification using maximum entropy principle and Akaike's information criterion, based on illustrative examples.

Chapter 4 gives a brief insight into field soil testing that was carried out at the Nipigon River landslide slope site.

Chapter 5 exhibits the reliability analysis of the Nipigon River landslide slope, which incorporates the developed modified first-order reliability method and its comparison with the GEO-Slope-based Monte Carlo simulation method in order to compute the reliability index and the probability of failure of the Nipigon River landslide slope.

Chapter 6 displays the reliability-based design methodology of different combinations of the pile-reinforced slope design of the failed Nipigon River landslide slope.

Chapter 7 manifests the conclusions and future recommendations for adopted research methods.

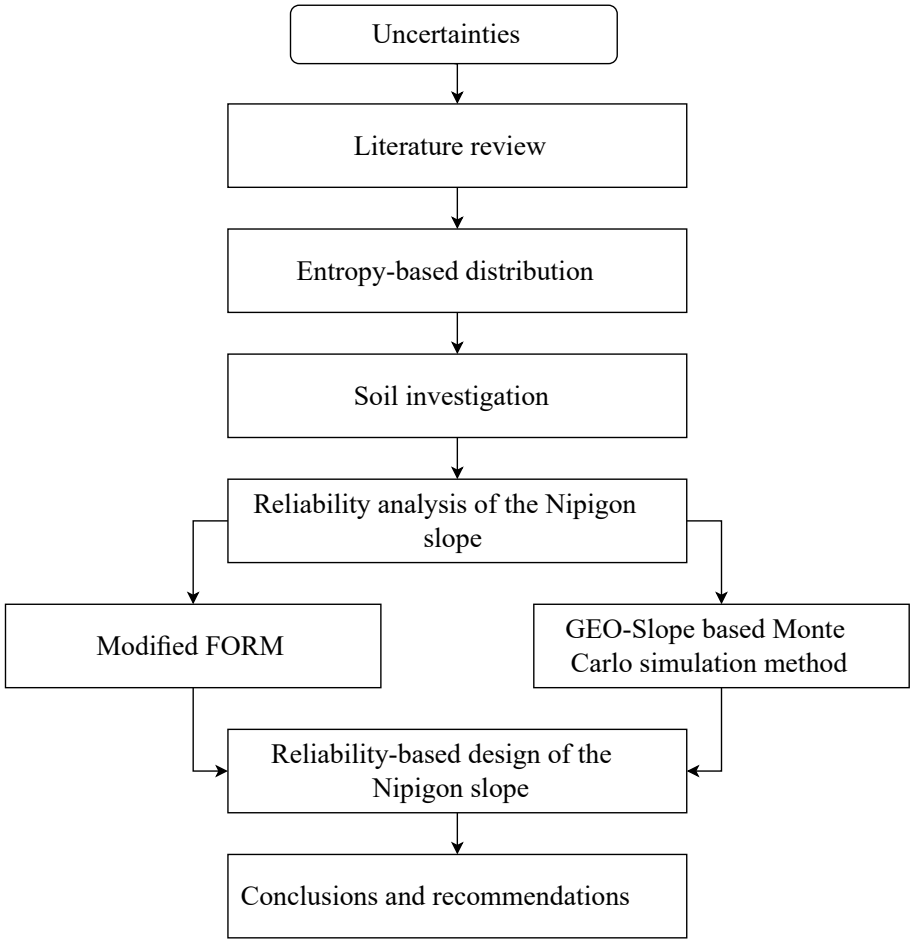

Figure 1.1: Flowchart depicting the structure of thesis

Chapter 2

Literature Review

2.1 Introduction

Slope stability has a significant role in the field of civil engineering. Stability analysis is carried out on a regular basis to compute the safety and functionality of various types of slopes. These slopes may be present in transportation facilities such as railroads, highways, airports, canals and many other human-made slopes (Huang, 2014). The slope stability analysis method is chosen based on the conditions of the site as well as the failure modes of the slope. Moreover, precise importance is given to the pros and cons of the adopted methodology (Shien, 2005).

It is well known that soil variables in slope engineering, similar to other geotechnical parameters, are bound to uncertainties, rendering it difficult to assess stope stability. These uncertainties include spatial variability in soil properties, geological incongruities, climatic and environmental conditions, drainage changes, analytical and computational errors, etc. Slope stability analysis is generally performed using conventional deterministic methods, which involve an overall factor of safety.

The deterministic approach is unable to explicitly account for various uncertainties associated with the slope. On the contrary, reliability analysis offers a systematic analysis of uncertainties and for their inclusion in evaluating slope performance. The proficient probabilistic framework al-

lows engineers and researchers to make a sound judgment in design and economical features of the slope.

2.2 Deterministic Slope Stability Analysis

The most frequently-adopted method for slope stability analysis is the limit equilibrium method. Based on the concept of Coulomb's failure criterion, a failure surface is assumed (Huang, 2014). The limit equilibrium state occurs when the shear stress along the failure surface is:

$$\tau = \frac{s}{F}, \tag{2.1}$$

where τ is shear stress, s is a shear strength, and F is a factor of safety. The shear strength for Mohr-Coulomb theory is:

$$s = c + \sigma_n \tan \phi, \tag{2.2}$$

where c is the cohesion, σ_n is the normal stress and ϕ is the friction angle (Huang, 2014). The shear stress can be determined by Eq. (2.2) after the factor of safety is calculated.

2.2.1 Method of Slices

This is the first approach to compute slope stability based on the limit equilibrium method, keeping in mind the mechanical equilibrium of forces and moments of the stresses acting on the sliding body mass (Priceputu, 2013). The methods of slices are convenient for hand calculations, therefore, they were first used for computing slope stability.

The fellenius method of slices is the most common and simplest approach to determining the linear equation of the factor of safety. In this

approach, the vertical and horizontal forces (i.e., the interslice forces) are assumed to be equal, and are neglected. The factor of safety evaluated by the fellenius method is conservative, and is almost 50% below the actual equilibrium value (Whitlow, 2000).

Janbu's simplified method is adequate for the arbitrary shape slip surfaces and is used very frequently, everywhere. Rigorous methods that satisfy both force and moment equilibrium equations are considered to be the best method, where Janbu's method falls behind. It relies upon the correction factor f_0 (Janbu, 1973) to account for the interslice shear forces like an angle of friction, cohesion and failure shape.

Compared to Janbu's simplified method, the rigorous method includes the interslice forces to compute the normal force on the base of the vertical slice. An iterative procedure is required to compute factor safety of equation, and therefore, problems of convergence of the numerical solution arise for some slip surfaces. This method often leads to an approximate solution due to the lack of the parameters introduced during analysis to balance some equations and unknowns (Fredlund & Krahn, 2011; Kenneth et al., 1983). S. Zhang (1990) developed a method in which the tension cracks are considered based on Janbu's method whereby the slip surface, having a large curvature, is neglected. This approach helped to eliminate the problem of convergence.

The Morgenstern method and Price method defines the interslice forces by assuming an arbitrary mathematical function:

$$\lambda f\left(x\right) = \frac{T}{E}, \tag{2.3}$$

where, λ is represented as the parameter to be computed, $f(x)$ is the horizontal coordinate, assumed function of x. To compute the factor of safety Morgenstern and Price combined the force equilibrium equations and then

used the Newton-Raphson method to calculate the moment and force equilibrium equations of the factor of safety and λ. This method is like Spencer's when the $f(x)$ is constant. Fredlund & Krahn (2011) developed an advanced modified Morgenstern and Price method because of the complications associated with the solutions.

In addition to the methods mentioned above, many other approaches have been developed by researchers. The contrast between the various methods based on the satisfaction of equilibrium conditions and assumptions for the problems are shown in Table 2.1.

Table 2.1: Element of the static equilibrium satisfied by various limit equilibrium methods (Shien, 2005)

Method	Horizontal Force	Equilibrium Vertical	Moment Equilibrium	Assumption
Ordinary or Fellenius	Yes	No	Yes	Inter-slice forces are neglected
Bishop's simplified	Yes	No	Yes	Resultant inter slice forces are horizontal
Janbu's method	Yes	Yes	No	Resultant inter-slice forces are horizontal, an empirical inter-slice factor is used to account for shear force
Spencer's	Yes	Yes	Yes	Resultant inter-slice forces are constant slope throughout the sliding mass
Morgenstern and Price method	Yes	Yes	Yes	Direction of the resultant inter-slice is defined using an arbitrary function. The percentage of the function is computed

2.2.2 Numerical Methods

Statistical simulations can deal with the uncertainties incorporated within the soil parameters. These can be used to quantify uncertainty and estimate the different outcomes of the likelihood of occurrence. Engineers can design more robust and economic structures, as well as solutions to problems. Numerical methods such as finite element, and discrete element methods, are frequently used in slope stability analysis (Griffiths & Lane, 1999).

Finite Element Method

The Lagrangian formulations of the finite element method have been adopted ever since the geometric non-linearity concept was developed in the calculation. Finite element method is a potent computer programming tool for computations in engineering. The finite element method is a potent computer programming tool for computations in engineering. It can simulate the actual physical behavior of the structure using computer programming tools, therefore avoiding any simplification in the process.

In the slope stability analysis using the finite element method, the same failure criteria as in limit equilibrium are used without making any assumptions. Many methods have been proposed during the past decades that rely upon finite element methods for slope stability analysis. The gravity increase method by Swan & Kyo (1999) and strength reduction method by Matsui & San (1992) are the most popular methods used until now. The gravity increase method functions by gradually increasing the gravitational forces until the slope fails, and then the factor of safety is calculated by the ratio of gravitational forces at failure to the actual gravitational acceleration. In the strength reduction method, the soil parameters are reduced so that the slope becomes unstable and eventually fails. In fact, Griffiths & Lane (1999) claimed that the strength reduction method is similar to the

limit equilibrium method.

Discrete Element Method

This method, also known as the Euler-Lagrange finite element method, has substantial computational complexity. Hence, it is still considered doubtful from an engineering point of view. The discrete element method has been adopted by many researchers in various fields of engineering. Cundall (1971) used the finite element method in a computer model to simulate the large-scale movement of blocky rock systems. Chang (1992) used the discrete element method to conduct slope stability analysis. His model was a slight extension of the traditional deterministic right plastic assumption, without the requirement of any assumptions regarding interslice forces (Chang, 1992). Chang concluded that the discrete element method used in the research was more rigorous than the deterministic approach, and the consideration of the elastoplastic.

2.2.3 Limitations of Deterministic Methods

The traditional method adopts the deterministic methodology. The factor of safety determines whether or not the slope is safe. If the value of the factor of safety is greater than 1, the slope is safe; if it is less than 1, the slope is unsafe. The factor of safety value also depends on the sound judgment of the engineer about the input parameters, failure mode, assumptions, and analysis methodology (Shien, 2005). Because the uncertainties associated with the system are neglected, the traditional approach is very unreliable and subjective (Liang et al., 2014; Dian Qing et al., 2017).

2.3 Uncertainties in Slope Stability Analysis

In the analysis and design of geotechnical structures, various sources of uncertainties are encountered, that are very well known (Abbaszadeh, Shahriar, Sharifzadeh, & Heydari, 2011). Morgenstern (1995) grouped the uncertainties into three categories. The flowchart 2.1 below displays the uncertainties associated with soil properties.

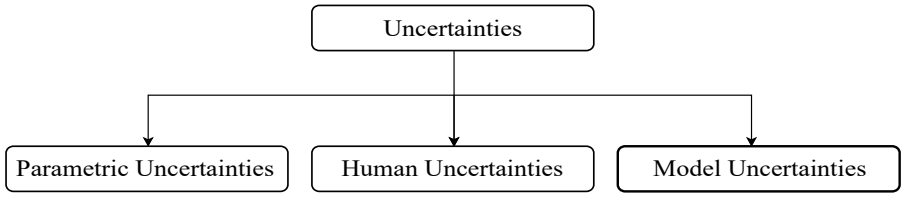

Figure 2.1: Uncertainties associated with soil parameters

2.4 Conventional Methods of Modelling Uncertainty

The most significant problem encountered in the probabilistic design approach is the ability to quantify the available information regarding the random variables. The information can be available in the form of sample values that may be computed from laboratory tests, field measurements, etc. Nevertheless, the information can have some uncertainties, and may be less explicit. Hence, there should be a way to incorporate this available information into the design.

2.4.1 Histogram and Frequency Diagram

The initial step in modeling the uncertainties is to consider the parameters of the soil to be random variables. Usually, the strength parameters such as cohesion (c), density (γ), angle of friction (ψ), etc. are considered to be the most significant random variables.

Descriptors of Randomness

Engineers have discovered that during the analysis and designing of engineering systems, there is an existence of uncertainty and variability. However, the traditional or the conventional approach considers these uncertainties to be deterministic while relying on a single factor of safety value (Haldar & Mahadevan, 2000). On the contrary, an innovative probabilistic approach is a better option to account for variabilities and uncertainties in slope stability analysis. The focus of this thesis is to develop an advanced methodology to carry out reliability analysis of slope stability. Hence, it is important to study some basic concepts associated with probabilistic analysis based on the combined effects of basic and advanced statistics.

Random Variable

Every quantity in the civil engineering aspect is considered as a random variable, which can be any variable that is subject to randomness. The International Society for Soil Mechanics and Geotechnical Engineering (ISSMGE) Technical Committee defines a random variable as "a quantity, the magnitude of which is not exactly fixed but rather the quantity may assume any of the number of values described by a probability distribution" (ISSMGE, 2004; Shen, 1984). A random variable can be considered as discrete random variable or continuous random variable depending upon pattern it follows.

Measure of Central Tendency and Uncertainty

The information regarding properties of the random variable that are essential in practical application, can be evaluated by measuring central tendency (mean) and variability (standard deviation) of the random variable (Griffiths & Lane, 1999).

2.4.2 Analytical Models to Quantify Randomness

The analytical representation of randomness can be computed in the form of probability density function (PDF) and cumulative density function (CDF) (Haldar & Mahadevan, 2000). A continuous random variables histogram is fitted with the probability density function. The mean of the PDF represents the best estimate of the random variable whereas, the standard deviation or coefficient of variation of PDF represents uncertainty in a random variable. Alternatively, the information regarding the variable can be presented by the cumulative distribution function (CDF), which represents that a variable will have the probability of value less than or equal to the given range of the value. The CDF is the integral of the PDF.

The distribution can be determined in several ways, including drawing a frequency diagram, plotting data on probability paper and conducting statistical tests known as goodness-of-fit tests (Haldar & Mahadevan, 2000). There are multiple distributions used for the computation of probability and reliability of structures or events. Distribution analysis could be carried out with the help of various computer programs available on the market today. MATLAB, Microsoft Excel, and QUATRO PRO are the most used software (Haldar & Mahadevan, 2000). In the present research both, MATLAB and ExceL are utilized to conduct the analysis.

Some of the distributions that are used for representing information in the form of PDF are the Normal distribution, Student's t-distribution, Chi-

square distribution, Poisson distribution, Exponential distribution, Binomial distribution, Rayleigh distribution, Beta distribution, Geometric distribution, Weibull distribution and Extreme value Type II and Type III (Haldar & Mahadevan, 2000). The limitation of this widely-used distribution method is that these methods result in a biased estimate of the mean, and are unable to provide insight regarding the population of distributions from which the computed data are a sample (Zhao & Frey, 2004).

2.4.3 Method of Probability Papers

The practical choice for the probability distribution may be made through mathematical formulations and knowledge about the distribution. In some cases, the distribution can be assumed to be uniform, triangular, trapezoidal, etc., whereas in other cases, more than one distribution can be fitted to a histogram with data information. Hence, sometimes the physical process of plotting data on probability paper may provide a specific form of the distribution (Haldar & Mahadevan, 2000). The distribution can be obtained by plotting the available information for random probabilities in the form of cumulative probabilities on suitable graph paper or probability paper.

2.4.4 Method of Moments

After the distribution for the particular random variable is obtained, the next step is to obtain the values of the parameters of the distribution. The parameters of different distributions are different in numbers depending upon the type of distribution. Distributions such as Binomial and Poisson have only one parameter, while others like log-normal and normal distribution have two parameters; many other distributions could have more than two parameters (Haldar & Mahadevan, 2000). The success of modeling uncertainty relies upon the accuracy of the parameter estimates based on the test

results. After the randomness is uniquely defined regarding the parameter of a distribution, the probabilistic analysis is carried out using these parameters.

The mean, or expected value, is considered as the first moment; variance represents the second moment, skewness represents the third moment, and so on. Hence, the method of moments concept can be adapted to estimate the parameters of distribution using information on its moments (Haldar & Mahadevan, 2000)

2.4.5 Statistical Tests

Even after plotting distributions on histogram or probability paper, the distribution does not provide a completely linear relationship, and distribution sometimes appears to be cumbersome. Therefore, more precise and definitive statistical goodness-fit tests can be applied to determine the distribution. Two of the most commonly-used statistical tests are Chi-square (χ^2) and Kolmogorov-Smirnov (K-S) tests. Chi-square tests based on the error between observed and assumed probability density function of distribution, whereas K-S test is based on the error between observed and assumed continuous density function of the distribution (Haldar & Mahadevan, 2000).

2.5 Distribution-free Method for Modelling Uncertainty

Distribution-free statistical methods are one that does not rely on presumptions of a known set of probability distribution function for their validity. If the validity of the method depends on the assumption that states the population distribution stems from an order of population probability distribution functions that are defined except for a finite number of parameters, then the

method is considered no longer as distribution-free (Conover, 2009).

In probabilistic approach , modelling and characterization of uncertainties in random variables are the first and the most significant step. This is because the subsequent reliability analysis of the structure is dependent upon the characterization of random variables. Uncertainties associated with the random variables are usually quantified by probability curves, mostly by probability distribution curves and its parameters. The conventional classical methods to compute the distributions and parameters from the available sample data, lack behind due to the restriction on the family of assumed standard theoretical distributions and susceptibility to sample sizes (Deng et al., 2004).

A more rationalized and convenient way to quantify the sample information is by evaluation of the sample moments. Maximum entropy principle has been adopted an a vital method for distribution fitting. The maximum entropy is based on Shannon's entropy, which is a measure of uncertainty that has been adopted in several disciplines of engineering for estimating distribution functions (Sobczyk & Trcebicki, 1999; J. Zhang & Gu, 2015; J. Li & Xu, 2011). The method will be explained in next chapter more precisely.

Maximum entropy generates the unbiased estimate of the probability density function, which signifies most probable or likely (PDF) from all the sets of density functions subject to moment constraints. In one of the studies, the maximum entropy method (MEM) was adapted to estimate the probability density function and evaluate the slope stability by C. Li et al. (2012), who adopted a fourth-moment procedure and maximum entropy principle utilization to conduct a reliability analysis for earth slopes. The aim of this research is to present a distribution -free approach , by combining maximum entropy formalism with Akaike's information criterion for

estimating the probability curves directly from field sample data and then carry out slope stability analysis.

Lindley (1956) was the first to apply information theory to quantify information produced by analysis based on the Bayesian approach. Commenges (2015) demonstrated the application of information theory in statistics, especially in bio-statistics.

Besides, Baker (1990) presented a procedure of estimation of probability density function based on information theory concepts. It combined Jayne's maximum entropy formalism with Akaike's information criterion for the selection of the optimal member of a group of model order. Baker validated his proposed method by its application on structural live loads, soil parameters, and the stochastic foundation design. Later, a concept of cross entropy was introduced by a refined approach to combine a prior distribution with available data (Deng & Pandey, 2009b, 2000; Sobczyk, 2003). In addition, Deng & Pandey (2009a) developed a rigorous quantile function being exceptionally fit for a small sample size using maximum entropy. Deng & Pandey (2008b) developed the estimation method, in which he combined the Monte Carlo simulations and optimization algorithms to compute fractionals of probability-weighted moments to generate the best-fit quantile function.

Hence, maximum entropy has been employed in various fields of engineering simultaneously with geotechnical engineering. In this research, an approach is proposed to conduct slope stability analysis based on combined distribution-free method of maximum entropy formalism, and Akaike's information criterion concept. Also, the first-order reliability method is modified to incorporate the non-normal parameters of MEF and AIC, and compute the reliability analysis of the Nipigon River landslide slope.

2.6 Probabilistic Slope Stability

Probabilistic methods are based on the risk-based design concept. Risk-based designs are non-uniform when applied to different engineering disciplines (Haldar & Mahadevan, 2000). Rather than using a single safety factor for resistance alone, it is more appropriate to apply the safety factor to a load as well as to resistance, i.e., load and resistance factored design (LRFD) (Haldar & Mahadevan, 2000). The risk can be measured on a probability of failure event or $P(R < S)$, where R is resistance and S is Load.

Slope engineering is linked to several uncertainties, such as the inherent spatial variability of the soil properties, subsurface uncertainties, and uncertainties due to modeling. Slope stability analysis by utilizing probabilistic and statistics theories provides a comprehensive approach to account for these uncertainties. Reliability of slope stability is recognized as the measure of the reliability index (β) or probability of failure of slope (p_f). Table 2.2 represents the (β) and (p_f) satisfactory performance level. The probability of failure of slope (p_f) and reliability index (β) can be assessed using several methods. These methods are addressed further in this section

Table 2.2: Probability of failure indices (Corps, 1999)

Expected Performance Level	Beta	p_f of Unsatisfactory Performance
High	5	0.0000003
Good	4	0.00003
Above average	3	0.001
Below average	2.5	0.006
Poor	2	0.023
Unsatisfactory	1.5	0.07
Hazardous	1	0.16

The first step to evaluating reliability or the probability of failure of a system is to set up a performance function; the parameters relationship as

per the performance function are known as variables X_i (Haldar & Mahadevan, 2000). The performance function is as:

$$Z = g(X_1, X_2...., X_n). \tag{2.4}$$

The failure surface or limit function can be defined as $(Z = 0)$ (Haldar & Mahadevan, 2000). The limit state represents the boundary between the safe and unsafe region.

2.6.1 First Order Second Moment Reliability Method

The uncertainty in this approach is taken as a function of the uncertainty in the model. The method follows the procedure of Taylor's series expansion of $g(X_1, X_2 \ldots X_n)$ around its mean value. The expected values or mean, as well as the standard deviation of the random variables, are used to evaluate mean and standard deviation of the performance function in the form of the factor of safety against slope stability (Haldar & Mahadevan, 2000). The result that we get from the FOSM is reliability index, β. The reliability index is the number of standard deviations of the performance function by which the mean value of the performance function goes more than the limit state (Shien, 2005). The FOSM method is described in the following steps by (Shien, 2005; Baecher & Christian, 2003).

1. Establish what variables result in uncertainty.
2. Compute the mean, variance, correlation coefficients, and auto-correlation distance of the random variables.
3. The determine the various distributions, spatially and systematically under uncertainty and then eliminate errors.
4. Calculate the mean of the performance function.

5. Determine the partial derivatives of the performance functions with respect to the random variables.
6. Get the contribution of random variables of the systematic and spatial variance of performance function.
7. Calculate the variance.
8. Compute the reliability index β, and probability of failure.

The advantage of the FOSM is that it helps in determining the degree of influence of the variables in uncertainty in a precise manner.

$$\beta = \frac{\mu_z}{\sigma_z}, \tag{2.5}$$

$$p_f = \phi(-\beta) = 1 - \phi(\beta). \tag{2.6}$$

μ_z is the mean and σ_z is the standard deviation. β denotes the reliability index and Eq. (2.6) gives the probability of failure. FOSM is instead a simplistic approach of slope stability analysis. In summary, FOSM is a simplistic approach of slope stability analysis, which requires a pre-defined critical slip surface of slope failure without accounting for the uncertainties correlated with the critical slip surface.

2.6.2 Point Estimate Method

An alternative method to FOSM was developed in 1981 (Rosenblueth, 1981). In the point estimate method, the probability distributions for continuous random variables are modeled by similar discrete distributions having more than or equal to two values (Shien, 2005). The discrete distributions elements have specific distributions with some values, the first few moments of these discrete distributions match the continuous random variables. Due to having fewer values for the integration, the performance function moments

are not difficult to compute.

In this procedure, the mean and variance are calculated using the weighted average of the discrete set of points in the uncertain parameter space. The moments of the performance function are determined by calculating the set of combined low and high values of the parameter (Shien, 2005). The complexity for computation increases with the number of uncertainty quantity of interests (Baecher & Christian, 2003). However, the approach is robust and accurate for a range of a practical problem. This method is straightforward, simple, direct and efficient for low order moment evaluation.

2.6.3 Monte Carlo Simulation

Monte Carlo simulation has been widely used to analyze slope stability (Tobutt, 1982), where randomly-generated points are used to cover the calculation values. This method is adopted when there is difficulty in solving the probabilities using analytical methods. Monte Carlo simulation is a robust method that can can compute system reliability (Haldar & Mahadevan, 2000). The procedure of this method is as follows (Shien, 2005).

1. The PDF of the random input variables is defined.
2. Based on the corresponding probabilities of the random variables, the pseudo-random numbers are generated.
3. The values generated are used to compute the performance function, and then the factor of safety is evaluated.
4. Large number of simulations are carried out to build up factor of safety.

The simulation numbers vary for each simulation model. The research conducted by Hutchinson & Bandalos (1997) revealed that for an appropriate result, 10,000 to 100,000 iterations are required. Its scope has recently

been enhanced due to advancement in the software. The explicit functions can be easily evaluated with its built-in software simulation technique, such as Excel's @Risk add-in. The software allows systematic reliability analysis of the entire system. The drawback of this software is that the distributions of the random variables should be known or assumed, which results in reduced accuracy of the distribution obtained for the performance function.

2.6.4 Reliability Judgment

The reliability index obtained from the analysis is more appropriate than the slope stability determined by a probability density function of factor of safety. It provides sound knowledge of the present condition of the structure or slope, as well as its future performance. Slopes with a higher value of reliability index are considered more reliable, and vice-versa. The slope with the low-reliability index is considered to be a hazard (Shien, 2005). Santamarina et al. (1992) developed criteria for assessing slope failure consequences, as shown in Table 2.3.

Table 2.3: Probability of failure criteria of slope (Santamarina, Altschaeffl, & Chameau, 1992)

Conditions	Criteria for Probability of failure
Temporary structures with low repair cost	0.1
Existing large cuts on interstate highway	0.01
Acceptable in most cases Except if life may be lost	0.001
Acceptable for all slopes	0.0001
Unnecessarily low	0.00001

2.6.5 Correlation of Variables

The probabilistic approach also computes correlation coefficients between different variables. They are mostly between the parameters such as friction angle, cohesion and unit weight. Table 2.4 represents co-variance values suggested by various researchers. The laboratory tests performed on different soils have provided results that cross correlation between angle of friction, and cohesion ranges negatively correlated between -0.72 and 0.35 (Shien, 2005).

Table 2.4: Coefficient of variance suggested by researchers (Shien, 2005)

Parameter	Coefficient of Variance $\%$	Reference
Unit weight	3, 4 to 8	Wolff (1996)
Drained strength of sand $\phi^{'}$	3.7 to 9.3, 12	Wolff (1994)
Drained strength of clay $\phi^{'}$	7.5 to 10.1	CD tests on compacted clay at Cannon dam, Wolff (1985)
Undrained strength of clay Su	40, 30 to 40, 11 to 45	Fredlund and Dahlman, Wolff (1994), UU tests on compacted clay at Canon Dam, Wolff (1985)
Strength to effective stress ratio, $\frac{Su}{\sigma_v}$	31	Wolff (1994)
Permeability of top blanket of clay, k_b	20 to 30	Wolff (1994)
Permeability of foundation sands, k_f	20 to 30	Wolff (1994)
Permeability ratio, $\frac{k_f}{k_b}$	40	Derived using 30% for k_f and k_b
Permeability of embankment sand, k_f	30	Wolff (1994)

2.7 Software for Slope Stability Analysis

There are various types of commercial software available on the market that are used for conducting slope stability analysis. Meanwhile, each procedure adopted in these commercial software packages is different. Some software carries out only deterministic slope stability analysis, while others are capable of both deterministic as well as probabilistic analysis of slope stability. Some software specifications are explained in the following subsections:

GEO5 geotechnical software suit software can be used for shallow foundation design, underground construction and tunneling, soil dynamics and earthquake engineering, rock mechanics, deep foundations, retaining walls, finite elements, soil mechanics, flow seepage and slope stability. GEO5 offers analytical and numerical approaches for solving problems related to the geotechnical field. It is developed by Fine spol.s r.o. AEC slope is used for analyzing the stability of slopes for roads, railways, river training works, canal embankments, dams, etc. AEC software works in tandem with AutoCAD application, and uses the method of slices such as the Swedish method of analysis for slope stability. It does not consider the pore water condition.

Galena software helps in determining the slope stability of soil and rock based on the deterministic methods such as Bishop (circular), Spencer-Wright (circular and non-circular) and Sarma. The model can include external forces acting on the slope, loads distributed on the slope and earthquake effects. Piezometric surface lines can be defined separately for each layer separately.

GEO-Slope SLOPE/W is the very efficient and very dynamic software used for the slope stability analysis. It is the most reliable and used by engineers and researchers all over the world (Melentijevic, Serrano, Olalla,

& Gao, 2017; Kang, Zerkal, Liu, Huang, & Tao, 2018). It can be used to analyze both simple and complex problems for a variety of slip surface shapes, pore water pressure conditions, soil properties, and loading effects. It includes pore water pressure defined lines using piezometric lines, rapid draw-down analysis and deterministic, and has a probabilistic slope stability analysis feature. The GEO-SLOPE 2007 software is used in the proposed slope stability analysis.

2.8 Reliability Based Design

The presence of uncertainties in either engineering computations or geotechnical variables demands a reliability-based design (RBD) approach for a robust and cost-efficient design. The random variables of the parameters are utilized as system-designed variables, where cost optimization is carried out using mathematical models subject to constraints (Wang, Hwang, Juang, & Atamturktur, 2013). The RBD design provides higher confidence level in design (Wang, Hwang, Juang, & Atamturktur, 2013). Many researchers have utilized the reliability index computed by the traditional reliability analysis method for design purpose(Enevoldsen, 1994; Enevoldsen & Sørensen., 1994; Allen & Maute, 2004). RBD approach was adopted by Wang et al. (2013), who included a robust geotechnical design approach to make the probability of failure insensitive to change in rock shear properties by adjusting the design variable parameters. In this thesis, the reliability index computed from the proposed probabilistic reliability analysis is used as initial design variables. Later, when the given constraint is not satisfied, design optimization is carried out by changing the design parameters accordingly in order to achieve the desired probability of failure

2.9 Summary

This chapter reviews the previous research on the geotechnical parameters quantification, uncertainties in the soil properties, deterministic slope stability analysis, and probabilistic slope stability analysis. Also, the chapter summarizes various software used for slope stability analysis. The understanding of the objectives mentioned above will be kept in view and modified while moving further into the proposed methodology of the present thesis.

Chapter 3

Entropy-Based Probabilistic Distribution of Soil Variables

3.1 Introduction

This chapter presents a new approach for estimating probability density function of soil variables in geotechnical engineering. The methodology is based on two-stage analysis, using Jayne's maximum entropy formalism and Akaike's information criterion. The approach provides a systematic analysis of the selection of an optimal member of the hierarchy of models (Baker, 1990). The analysis is based on the continuous random variable with continuous probability functions and unknown finite moments. The method is universal in nature, which results in distribution-free modelling of soil variables. Lastly, methodology is illustrated by its application on data in examples.

The structure of the chapter is as follows. In Section 3.2, the theory of maximum entropy formalism is described. Section 3.3 derives Akaike's information criterion application to the maximum entropy formalism. Section 3.4 presents examples, and a summary is presented in Section 3.5.

3.2 Maximum Entropy Principle

The probability distributions of the random variable can be possible, under certain circumstances by using Jayne's principle (Rosenkrantz & Baierlein, 1984). But the classical formulation of this formalism assume the availablity of a set of population moments, and hence can not be applied to most engineering problems. To overcome this issue Baker (1990) combined Jayne's MEF with Akaiki's information criterion. The method is able to deal with the type of problems encountered in civil engineering.

Both MEF and AIC are here as two different aspects of minimization of Kullback-Leibler relative entropy (Baker, 1990). This approach is a Bayesian approach, and therefore requires a precise definition of the prior information. In the present research it is assumed that random variable X is bounded interval $x_{min} \leq x \leq x_{max}$ where x_{max} and x_{min} represents prior information.

In the information theory entropy represents a quantitative measure of the information content of a probability distribution function (Baker, 1990). While in the present analysis this approach is applied to measure the information regarding uncertainties associated with random variables in civil engineering.

The maximum entropy approach is based on the concept of entropy, which is defined as a quantitative information content of a probability distribution function. Under this mechanism, the distributions with a flat shape are considered less informative than the narrow peaked one.

Kullback's Entropy Functional

The information theory in statistics was introduced by Kullback & Leibler (1951) and presented in his book on statistics (Lindley, 1959). In the field

of statistics, entropy is the measure of uncertainty. Kullback's entropy functional helps to determine the measure of entropy measure between two probabilities. The true measure of information content for a discrete random variable can be computed using Shannon entropy (Baker, 1990).

$$H[P(x)] = -\sum_{i=1}^{n} P(x_i) \ln[P(x_i)], \tag{3.1}$$

where $P(x)$ is the probability of the random variable X will have the value x, and with total n number of possible values of X. Shannon's entropy cannot be defined for continuous random variables because the value obtained from this measure approaches infinity in the process of transformation from discrete to continuous case (Baker, 1990). However, the entropy difference between two distribution is finite, and can be computed by using Kullback-Leibler information function $H[p_1(x), p_2(x)]$ (Lindley, 1956). The function enables to measure the entropy difference between two probability assignments $p_1(x)$ and $p_2(x)$. The function is given as:

$$H[p_1(x), p_2(x)] = \int_D p_1(x) \ln \left[\frac{p_1(x)}{p_2(x)}\right] dx, \tag{3.2}$$

where D is the range of the random variable X. The important aspects of Kullback's entropy function are:

- $H[p_1(x), p_2(x)]$ is invariant to all monotonic transformations of the random variable X
- $H[p_1(x), p_2(x)] \geq 0$ for all possible distribution functions $p_1(x)$ and $p_2(x)$.
- $H[p_1(x), p_2(x)]$= 0, defines that $p_1(x) = p_2(x)$.

These relations are depicted in (Baker, 1990).

Jayne's Maximum Entropy Formalism

Jayne states that "the minimally prejudiced assignment of probabilities is one which minimizes the entropy subject to the satisfaction of the constraints imposed by the available information" (Rosenkrantz & Baierlein, 1984). Therefore, considering $H[P(x), P_0(x)]$ as the information measure, Jaynes' principle signifies that the best probability assignment $p(x)$ is the solution of Eq. (3.3). Minimize

$$H[p(x), p_0(x)] = \int_D p(x) \ln[\frac{p(x)}{p_0(x)}]dx, \tag{3.3}$$

subject to satisfaction of constraints:

$$p(x) \geq= 0 \quad \forall_x \in D, \tag{3.4}$$

$$\int_D p(x)dx = 1, \tag{3.5}$$

$$I_k[p(x)] = 0 \quad k = 1, 2, ..., K, \tag{3.6}$$

where $p_0(x)$ is the prior distribution of X and $I_k[p(x)] = 0$, $k = 1, 2, .., K$ is a set of K constraints defining the available information. Jayne's principle is based on the mechanism to take the best probability assignments as close as possible to the prior distribution without contradicting the available physical information in Eq. (3.6) and other basic requirements of density function in Eqs. (3.4),(3.5). The importance of Jayne's contribution is that Shannon's and Kullback's entropies are the measures of the distance between probability distributions in discrete and continuous cases, respectively. Jayne's defined the entropy as $-H[p_1(x), p_2(x)]$ and maximized this equation, therefore it is know as 'maximum entropy formalism'. The set

of constraints represented in Eq. (3.6) is to assume K population moments $\mu_k, \quad k = 1,...,K$

$$I_k[p(x)] = \mu_k - \int_D x^k p(x)dx = 0 \quad k = 1, ..., K. \tag{3.7}$$

The solution of the minimization problem in Eq.'s (3.3), (3.5) and (3.7) is follows:

$$p_k(x|\mu) = p_0(x) \exp\Big[Z_0 + \sum_{k=1}^{k} \lambda_k x^k\Big], \tag{3.8}$$

where, λ_k, k = 1,...,K is a set of Lagrangian multipliers associated with the physical constraints Eq. (3.8), Z_0 is the multiplier associated with normalization constraint in Eq. (3.5), and $\mu = (\mu_1, ..., \mu_K)$ is the vector of given population moments. The notation $p_k(x|\mu)$ represents the importance that Eq. (3.8) corresponds to a given vector of population moments. By substituting Eq. (3.8) in the Eq. (3.5) we get:

$$Z_o = -\ln\Big\{\int_D p_0(x) \exp\Big[\sum_{j=1}^{k} \lambda_j x^j\Big] dx\Big\}. \tag{3.9}$$

This equation shows that the Z_0 is fixed by the Lagrangian multipliers $\lambda = (\lambda_1, \lambda_2, \lambda_3, \lambda_k)$.

Substituting Eq. (3.8) and (3.9) into Eq. (3.7) we can compute the values of λ from the following equation:

$$\frac{\int_D x^k p_0(x) \exp\Big[\sum_{j=1}^{K} \lambda_j x^j\Big]}{\int_D p_0(x) \exp\Big[\sum_{j=1}^{K} \lambda_j x^j\Big]} = \mu_k \quad k = 1, ..., K. \tag{3.10}$$

Considering the maximum entropy distribution $p_k(x|\mu)$ as a model, the L.H.S of Eq. (3.10) signifies the theoretical model moments (μ^M). In the end, Eq. (3.8) is substituted in Eq. (3.3) using the constraints in Eqs. (3.5)

and (3.7), to get the solution of entropy of optimal order $p_k(x|\mu)$ (Baker, 1990):

$$H[p_k(x|\mu), p_0(x)] = \Big[Z_0 + \sum_{k=1}^{k} \lambda_k \mu_k\Big]. \tag{3.11}$$

If X is a random variable of any parameter and $x_1 ... x_N$ are the N measured values for data set rather than set of population moments. It is possible to calculate N independent sample moments $\widehat{\mu}_k$, k = 1,..., N as:

$$\widehat{\mu}_k = \frac{1}{N} \sum_{j=1}^{N} [x_j]^k k = 1, ..., N \tag{3.12}$$

The density $p_k(x|\mu)$ defined in Eq. (3.8) for the unknown values of population moments, signifies a family of distributions parametrized by the K unknown constants $\mu = \mu_k$, $k = 1, ..., K$. As Eqs. (3.9) and (3.9) show that $\mu = f(\lambda)$, and Z_0 = $f(\lambda)$, it is possible to take Lagrangian multipliers as the unknown parameters of distribution in place of μ and write $p_k(x|\lambda)$ for the Kth order Maximum Entropy Family of Distributions (MEFD). Baker (1990) stated that the search of probabilistic models using the MEFD does not result in any loss with respect to the shape of the probability distributions.

3.3 Akaike's Information Criterion

With Jayne's maximum entropy formalism a family of distributions with parameters was established in Eq. (3.8). The further step after establishing Eq. (3.8) of the family of distribution is to compute both the number of parameters and their values, which depicts the information present in the sample. Akaike (1973) and others provided a solution to such a problem (Baker, 1990). Let $g(x)$ be the unknown distribution and $p_k(x|\lambda)$ be Kth

order model. The measure of distance between $p_k(x|\lambda)$ and $g(x)$ is represented in the Kullback-Leibler entropy in Eq. (3.13).

$$H[g(x), p_k(x|\lambda)] = \int_D g(x) \ln \Big[\frac{g(x)}{p_k(x|\lambda)}\Big] d(x), \tag{3.13}$$

The best choice for λ is minimizing the distance between $p_k(x|\lambda)$ and $g(x)$. Since, $g(x)$ is not known, we are unable to evaluate the L.H.S of Eq. (3.13). Eq. (3.13) can be re-written as:

$$H[g(x), p_k(x|\lambda)] = C - L(\lambda, K), \tag{3.14}$$

where:

$$C = \int_D g(x) \ln[g(x)] d(x), \tag{3.15}$$

and,

$$L(\lambda, K) = \int_D g(x) \ln[p_K(x|\lambda)] dx. \tag{3.16}$$

The term C does not depend on λ, hence while minimizing H with respect to λ this C term is constant. It is evident from Eq. (3.16) that $L(\lambda, K)$ is the expected value of $\ln[p_K(x|\lambda)]$, therefore from N measurements of sample, we can obtain natural estimate $\widehat{L}(\lambda, K)$ of $L(\lambda, K)$.

$$\widehat{L}(\lambda, K) = \frac{1}{N} \sum_{j=1}^{N} \ln \Big[p_K(x_j|\lambda)\Big], \tag{3.17}$$

where x_j; j =1,...,N signifies N measured sample values. The estimate of $\widehat{H}$ of H is:

$$\widehat{H}(\lambda, K) = C - \widehat{L}(\lambda, K) = C - \frac{1}{N} \sum_{j=1}^{N} \ln \Big[p_K(x_j|\lambda)\Big], \tag{3.18}$$

and the best choice of λ is computed by minimizing $\widehat{H}$ with respect to vector of unknown parameters λ.

$$\min_{\lambda}\Big\{\widehat{H}(\lambda,K)\Big\} = C - \frac{1}{N}\max_{\lambda}\Big\{\sum_{j=1}^{N}\ln\Big[p_K(x_j|\lambda)\Big]\Big\}. \tag{3.19}$$

The term $\sum_{j=1}^{N}\ln\Big[p_K(x_j|\lambda)\Big]$ is log likelihood function. Therefore, from equation Eq. (3.24) are maximum likelihood estimates (Baker, 1990). Akaike (1973) suggested that a best estimate of λ can be obtained if we maximize not the natural estimate $\widehat{L}$ of the biased likelihood function, rather an unbiased estimate of this function. The unbiased estimate is given as:

$$\widehat{L}(\lambda,K) = \widehat{L}(\lambda,K) - \frac{K}{N}, \tag{3.20}$$

hence, an unbiased estimate $\widehat{H}$ of H as in Eq. (3.21):

$$\widehat{H}(\lambda,K) = C - \widehat{L}(\lambda,K) + \frac{K}{N}. \tag{3.21}$$

The bias term K/N is directly proportional to model order K, which is the number of parameters that we try to estimate, and is inversely proportional to the number of sample data N. Akaike's information criterion can now be used for minimizing the Eq. (3.22).

$$\widehat{H}(\lambda,K) = C - (\frac{1}{N})\sum_{j=1}^{N}\ln[p_K(x_j|\lambda)] + \frac{K}{N}. \tag{3.22}$$

Eq. (3.22) can be summarize the Akaike's estimation procedure, that for a given value of K, minimize the unbiased estimate of the entropy given in Eq. (3.22), and get the optimal values of the parameters λ. Compute the entropy related to the best K th order model utilizing Eq. (3.22). Now λ_k is known so $\widehat{H}(\lambda,K)$ = $\widehat{H}(K)$ is a function of K only. Find the optimal

order approximation which minimizes the value of $\widehat{H}(K)$ as function of K:

$$min_K \widehat{H}(K) = K_{opt} \tag{3.23}$$

Akaike (1973) presented this program to determine the optimal model order of probability assignments (Baker, 1990).

3.3.1 Application of AIC to Family of Maximum Entropy

Akaike's information criterion and Jayne's maximum entropy formalism supplement each other. Both AIC and MEF are a Bayesian approach, and are based on the Kullback-Liebler minimization of information function. Hence, it is natural to apply the AIC procedure to the family of maximum entropy. In order to get combined explicit equation of AIC and maximum entropy, Eq. (3.8) and (3.22) are combined to get Eq. (3.22):

$$\widehat{H}(\lambda, K) = C - (\frac{1}{N}) \sum_{j=1}^{N} \ln[p_0(x_j)] - Z_0(\lambda, K) - \sum_{k=1}^{K} \lambda_k \Big[\frac{1}{N} \sum_{j=1}^{N} (x_j)^k\Big] + \frac{K}{N}, \tag{3.24}$$

The term $\sum_{j=1}^{N} \ln[p_0(x_j)]/N$ is independent of λ and K, hence it can be added in the constant C. The term $[\frac{1}{N} \sum_{j=1}^{N} (x_j)^k]$ represents the sample moments $\widehat{\mu_k}$, Eq. (3.24) becomes:

$$\widehat{H}(\lambda, K) = C - Z_0(\lambda, K) - \sum_{k=1}^{K} \lambda_k \widehat{\mu_k} + \frac{K}{N}, \tag{3.25}$$

to eliminate the constant C from Eq.(3.25), notice that for $K = 0$, also $Z_0 = 0$, gives:

$$\widehat{H}(K = 0) = C, \tag{3.26}$$

now,

$$\Delta H(\lambda, K) = \widehat{H}(\lambda, K) - \widehat{H}(K = 0) = \frac{K}{N} - Z_0(\lambda, K) - \sum_{k=1}^{K} \lambda_k \widehat{\mu_k}. \quad (3.27)$$

Eq. (3.27) is the differential entropy equation. This equation result can be either positive or negative, and it is not invariant to monotonic transformations (Baker, 1990). The optimal order parameters λ_K could be identified either by solving the nonlinear Eqs. (3.2) or by direct minimizing of $\Delta H(\lambda, K)$ using Eqs. (3.27), (3.9).

Advantage of the New Entropy Distribution

This approach is a distribution-free method, as no classical theoretical distributions were considered in advance (Deng, Pandey, & Xie, 2012; Deng & Pandey, 2010). The results provide a universal form of probability curves as per the implemented constraints. The method produces different distributions according to the given constraints, as shown in Table 3.1. The distribution obtained by maximum entropy is said to be the most unbiased, as it is derived from a systematic maximization of uncertainty about the unknown information (Deng & Pandey, 2009c). Therefore, this justifies the adopted approach, where the uncertainty is maximized by minimizing the distance between two probability assignments, i.e., prior probability and current information. This approach is a distribution-free method for estimating the models of random variables (Deng & Pandey, 2008a, 2009c; Deng, Pandey, & Gu, 2009).

Table 3.1: Maximum entropy probability distributions (Harr, 1987).

Given Constraints	Assigned Probability
$\int_a^b f(x)dx = 1$	Uniform
$\int_a^b f(x)dx = 1$ Expected value	Exponential
$\int_a^b f(x)dx = 1$ Expected value, standard deviation	Normal
$\int_a^b f(x)dx = 1$ Expected value, standard deviation, range (minimum and maximum values)	Beta
$\int_a^b f(x)dx = 1$ Mean occurrence rate between arrivals of independent events	Poisson

3.3.2 K-S Goodness-of-Fit Test

A goodness-of-fit test is generally used to measure the accuracy of the model fitted over the observed data. K-S goodness-of-fit method is being used to check the accuracy of models developed by maximum entropy method in further analysis.

Hypothesis Testing:

Let x_1,....,x_n be an ordered sample with $x_1 \leqslant ... \leqslant x_n$. $S_n(x)$ is given by Eq. (3.28):

$$S_n(x) = \begin{cases} 0, & x < x_1 \\ k/n, & x_k \leqslant x \leqslant x_{k+1} \\ 1, & x \geqslant x_n, \end{cases} \tag{3.28}$$

Now the $F(x)$ be the cumulative distribution function of the sample and D_n is a random variable, which is given by Eq. (3.29):

$$D_n = \max_x |F(x) - S_n(x)|, \tag{3.29}$$

where $F(x)$ is the theoretical CDF of the assumed distribution of the sample order x, and $S_n(x)$ is the corresponding stepwise CDF of the observed samples.

The objective is to use D_n as a way to estimate $F(x)$. The critical values of the distribution can be found from the Kolmogorov-Smirnov Table from Haldar & Mahadevan (2000). $D_{n,\alpha}$ is the critical value obtained from Table Haldar & Mahadevan (2000).

Now, D_n can be utilized to test the hypothesis of a sample of a specific distribution function $F(x)$ by Eq. (3.30) (Haldar & Mahadevan, 2000):

$$D_n = \max_x |F(x) - S_n(x)| \leqslant D_{n,\alpha}. \tag{3.30}$$

3.4 Illustrative Examples

Some examples are used in this section to illustrate the maximum entropy formalism and AIC procedure and its accuracy of distribution-free model fitted on basalt rock data and warehouse live load data. Firstly, OP-basalt and AM-basalt samples of uniaxial compressive strength parameters distribution free model is set up utilizing the proposed MEF and AIC. Secondly, sample data of warehouse live load is modelled using the adopted approach.

3.4.1 Basalt Rock Uniaxial Compressive Strength Parameter Modeling

The analysis is carried out on the rock mechanical parameters obtained from the tests results. The values of basalt rock uniaxial compressive strength parameter values are taken from a paper written by Cui et al. (2017). The proposed approach of the principle of maximum entropy formalism, along with Akaike's information criterion, is applied over a decent sample of 48 oblique porphyritic basalt (OP-basalt) uniaxial compressive strength parameter values. This approach provides the most unbiased and distribution free optimal model order of the parameter values.

Basalt is a basic rock, which consists of amygdaloidal structure and porphyritic texture and contains a wide variety of mechanical properties. Therefore, the inhomogeneous variability of natural rocks encounters uncertainties in the parameters obtained from laboratory testing (Cui et al., 2017). The present approach applies the uncertainties associated with these parameters to model the samples of uniaxial compressive strength parameters. Parameter modelling of 48 OP-basalt uniaxial compressive strength parameters is carried using the proposed methodology.

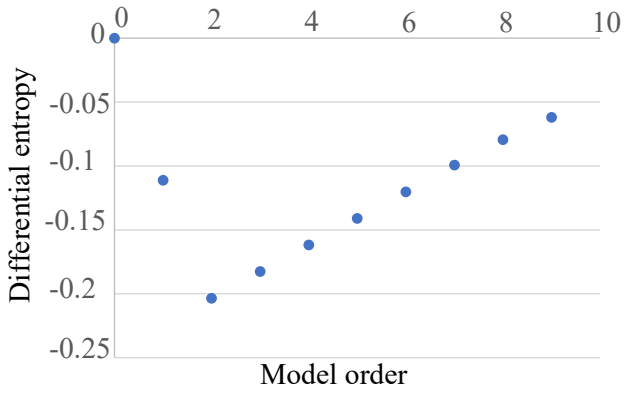

Figure 3.1: Differential entropy DH(K) of 48 OP-basalt uniaxial compressive strength parameter

Figure 3.1 displays the differential entropy graph with values for different model orders in transformed domain with $x_{min} = 0$ and $x_{max} = 50$. Inspection of the Figure 3.1 represents that 2nd model order has the minimum value of differential entropy out of all the other model orders. Consequently, having the minimum differential entropy value, 2nd order model is considered as an optimal order for the data of 48 OP-basalt uniaxial compressive strength parameter.

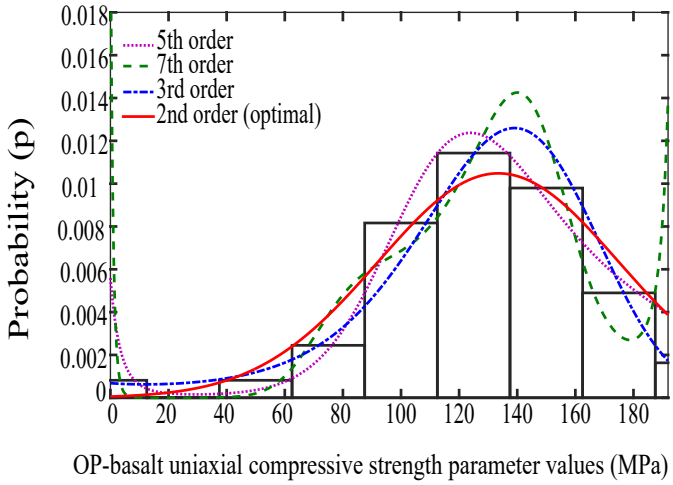

Figure 3.2: Data and density functions of 48 OP-basalt uniaxial compressive strength parameter

The values of 48 OP-basalt uniaxial compressive strength parameter sample data are given in Table 7.3. Comparing different models fitting the sample data of 48 OP-basalt in Figure 3.2, it is evident that almost all the model orders nicely fit the histogram of data. Looking at the 2nd model order (bold red line) and 3rd model order (dashed-blue line), both fit perfectly on the data except between range 40 to 70, where the 2nd model order has a slightly better fit than the 3rd order. Analyzing 7th order (broken-green line) and 5th order (dotted-pink line), these models fit fairly good on data

range between 80 and 180, but at the same time looks not very good fitting between the 40 to 70 range. Therefore, it can be deducted that 2nd order model is best for the overall data fitting.

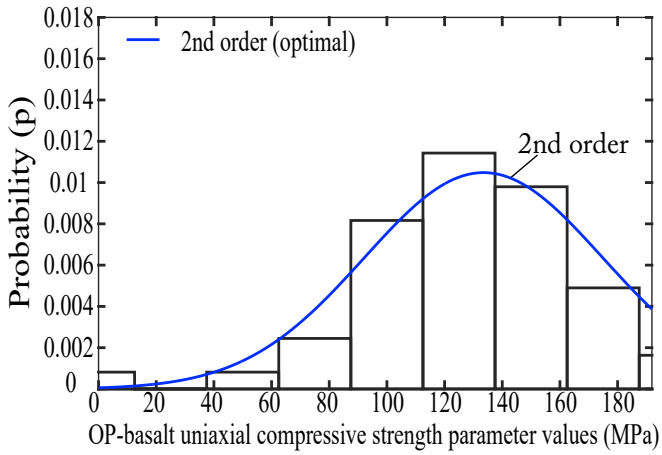

Figure 3.3: 2nd model order (Optimal) PDF for 48 OP-basalt uniaxial compressive strength parameter

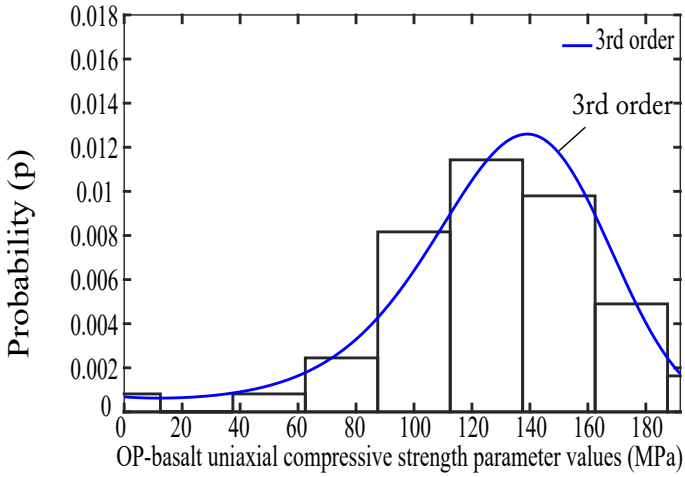

Figure 3.4: 3rd model order PDF for 48 OP-basalt uniaxial compressive strength parameter

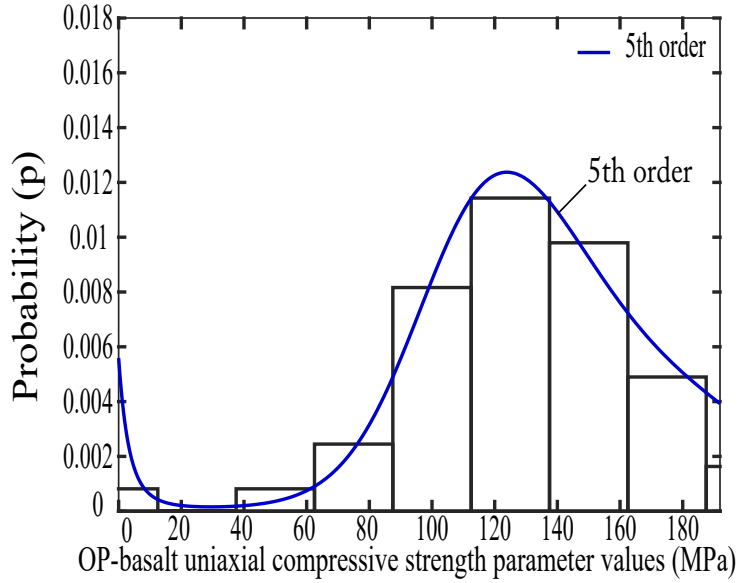

Figure 3.5: 5th model order PDF for 48 OP-basalt uniaxial compressive strength parameter

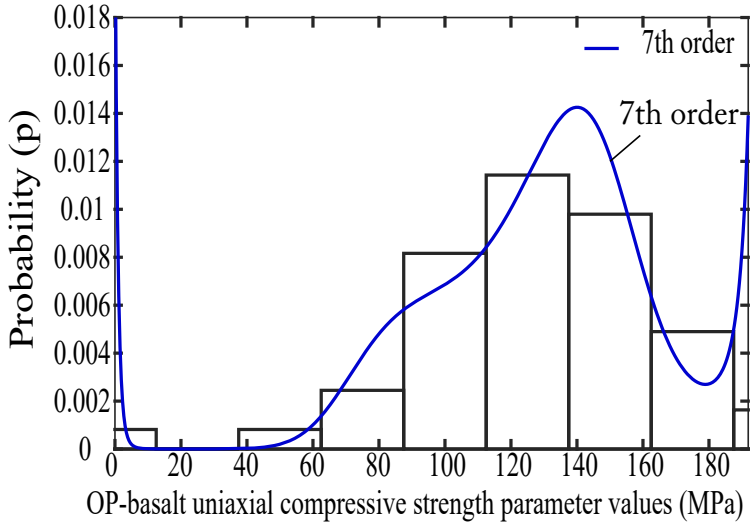

Figure 3.6: 7th model order PDF for 48 OP-basalt uniaxial compressive strength parameter

Table 3.2: Model parameters values of OP-basalt uniaxial compressive strength parameter

Model Order	Parameter (λ) Values
2nd(OPTIMAL)	$\lambda 1$ = -9.771160992862491, $\lambda 2$ =0.078094908026394, $\lambda 3$ =-0.000292475959781
3rd	$\lambda 1$ =-7.290924022675076,$\lambda 2$ = -0.014624183627745, $\lambda 3$ = 0.000662875259812, $\lambda 4$ =-0.000002925950626
5th	$\lambda 1$ =-5.186513805978763, $\lambda 2$ =-0.290221936748044, $\lambda 3$ = 0.007564130230584, $\lambda 4$ =-0.000070108541323, $\lambda 5$ =0.000000280675304, $\lambda 6$ =- 0.000000000416535
7th	$\lambda 1$ =-3.764815697547499, $\lambda 2$ =-1.172876317134412, $\lambda 3$ =0.047575602061369, $\lambda 4$ =-0.000772595215666, $\lambda 5$ =0.000006112759494, $\lambda 6$ =-0.000000022757465, $\lambda 7$ =0.000000000026889, $\lambda 8$ =0.000000000000023

Figures 3.3, 3.4, 3.5 and 3.6 present a view of the various model orders of entropy PDF fit on the data of 48 OP-basalt uniaxial compressive strength parameter values. It is seen that the curves of all model orders almost curve fit the histogram, other than between the range of 40 to 70, where the 2nd order is a better fit than the other model orders. Therefore, it is wise to consider the 2nd order as an optimal order with its perfect structure, as well as a differential entropy being best among all other model orders. Table 3.2 shows parameter λ values of optimal model order, as well as other model orders. Determination of the 2nd order model as a good fit over data is achieved by Kolmogorov-Smirnov goodness-of-fit test using an Excel spreadsheet and MATLAB.

In Table 3.3, columns 1 and 2 contain the data and their frequency. Column 3 depicts the identical cumulative frequency values, and column 4 divides these values by the size of the sample 48. Column 5 outlines the values of CDF acquired using the MATLAB program. Column 6 shows

eventually the variation between the values in column 5 and column 6. D_n implies the greatest value in column 6. The critical value of $D_{n,0.05}$ is obtained from Haldar & Mahadevan (2000). Considering that the value of D_n is less than $D_{n,0.05}$, we can resolve that the distribution data is a good fit with the 2nd model order of entropy distribution.
The density function $f(y)$ for a random variable y of the 2nd order is computed by applying the algorithm of maximum entropy formalism,

$$f(y) = exp(-9.771160992 + 0.078094902y - 0.000292475y^2). \quad (3.31)$$

Kolmogorov-Smirnov Test

Table 3.3: K-S goodness-of-fit test of 2nd entropy order on 48 OP-basalt

Data	Freq.	Cum freq.	$S_n(x)$	$F(X)$	Difference
0-20	0	0	0	0	0
21-40	0	0	0	0	0
41-60	0	0	0	0	0
61-80	3	3	0.062	0.073	0.011
81-100	5	8	0.166	0.208	0.042
101-120	11	19	0.395	0.401	0.006
121-140	11	30	0.625	0.611	0.014
141-160	10	40	0.833	0.787	0.046
161-180	6	46	0.958	0.900	0.058
181-200	2	48	1	0.921	0.079
					$D_n = 0.07$
					$D_{n,48,0.05}$= 0.1924

3.4.2 Warehouse Loads

This example is analyzed by Baker (1990) for an extensive data set. The measured values of load on the warehouse floor from Table 7.4 are used to explain the two-stage procedure of the maximum entropy formalism and

Akaike's information criterion. The results of maximum entropy with various model orders and their parameter values are shown in Figures below.

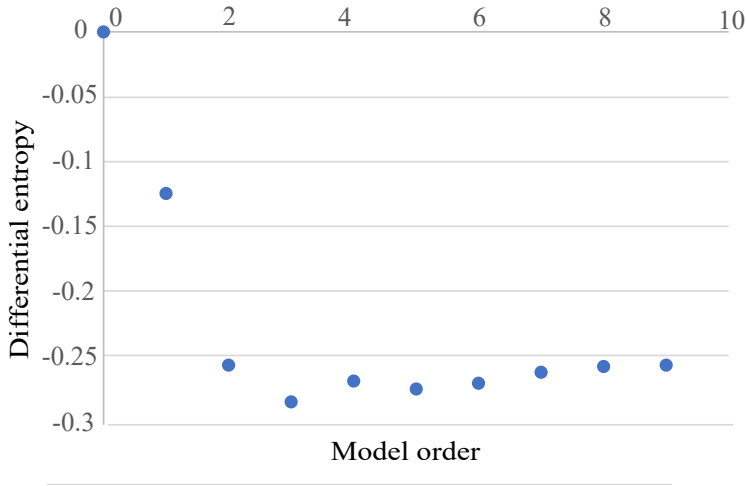

Figure 3.7: Differential entropy DH(K) of 220 sample of loads on the warehouse floor based on different model orders

Inspection of the Figure 3.7 shows the differential entropy graph with values for different model orders in transformed domain with $x_{min} = 0$ and $x_{max} = 250$. Figure 3.7 depicts that the 3rd model order has the minimum value of differential entropy. Hence, the 3rd order model is the optimal order.

Figure 3.8 shows the histogram of the data of load on warehouse. Figure 3.8 consist of four superimposed density functions; the 2nd order shown as a yellow dotted line, the 9th order in broken blue line, the 5th order as a green dashed line and the 3rd model, which is optimal order, is shown in solid red. The box in Figure 3.8 represents the values of λ, which are parameters of the optimal 3rd order.

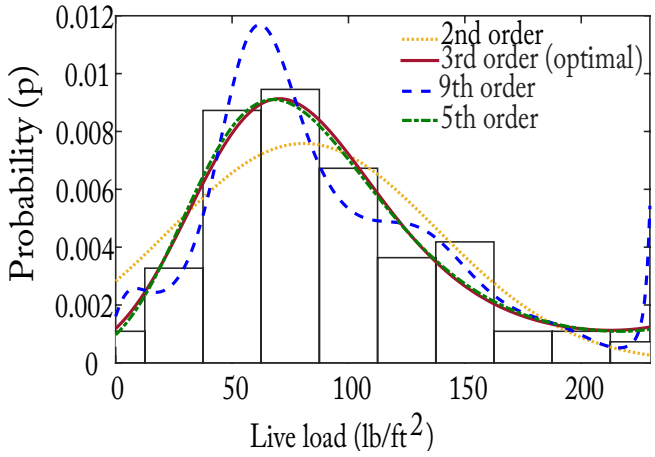

Figure 3.8: Data and density functions of 220 sample of loads on the warehouse floor

Figure 3.8 depicts that 3rd order model fits better than the 9th order model. When an optimal 3rd order is compared to the 2nd order, figure shows that 3rd order fits far more precisely than 2nd order model. Therefore, it is reasonable to choose the 3rd order rather than any other model order as an optimal model order. The 5th model fits the histogram very similar to optimal third order. One may conclude that the 3rd order as the optimal one as it has the lowest differential entropy.

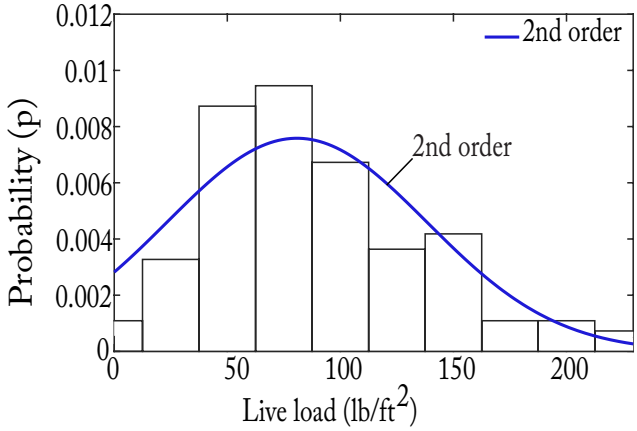

Figure 3.9: 2nd model order PDF for live load data

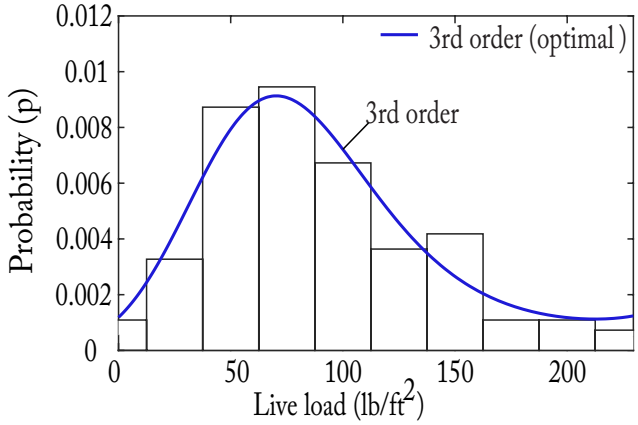

Figure 3.10: 3rd model order (optimal) PDF for live load data

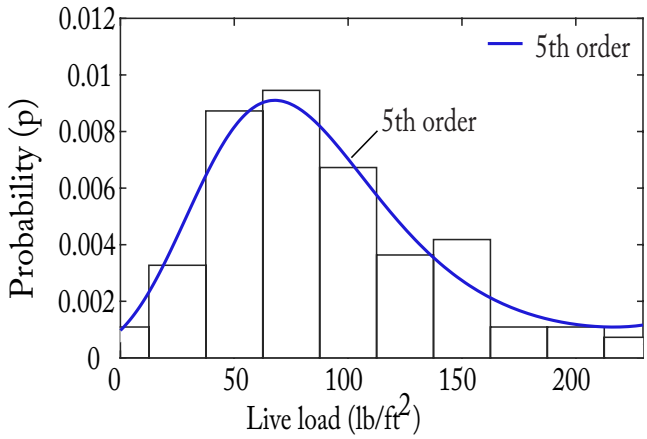

Figure 3.11: 5th model order PDF for live load data

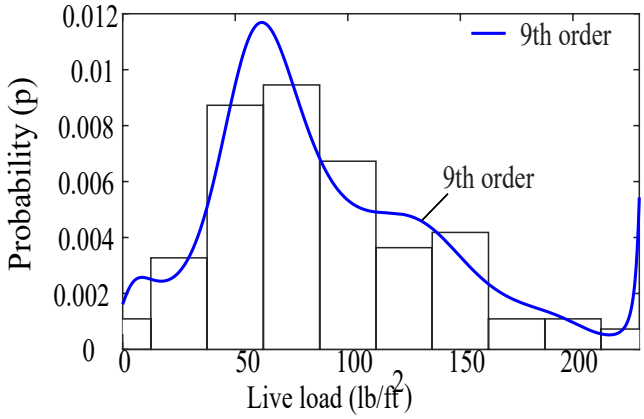

Figure 3.12: 9th model order PDF for live load data

Figures 3.9, 3.10, 3.11 and 3.12 show various model orders entropy PDF fit on the data of 220 live loads samples. It is evident that after reviewing different model orders curve, that the 3rd and 5th order models fit the histogram much better than the other two. However, when the 3rd order is compared with the 5th order in Figure 3.8, the 3rd order fits slightly better between range 0 to 20. Hence, the 3rd order is considered the optimal order.

Table 3.4: Model parameters values of warehouse live loads

Model Order	Parameter (λ) Values
2nd	$\lambda 1$ = -5.870793542437816, $\lambda 2$ = 0.024482080349970, $\lambda 3$ = - 0.000151473047107
3rd (OPTIMAL)	$\lambda 1$ = -6.737850943703387, $\lambda 2$ = 0.065287683515044, $\lambda 3$ = -0.000617917010756, $\lambda 4$ = 0.000001456554343
5th	$\lambda 1$ =-6.938032453466859, $\lambda 2$ =0.081466859694262, $\lambda 3$ =-0.000996520756702, $\lambda 4$ =0.000005066513981, $\lambda 5$ =-0.000000014872479, $\lambda 6$ =0.000000000021965
9th	$\lambda 1$ =-6.431565471459113, $\lambda 2$ =0.148780017319791, $\lambda 3$ =-0.016643428806383, $\lambda 4$ =0.000806707783746, $\lambda 5$ =-0.000018780382464, $\lambda 6$ =0.000000240246961, $\lambda 7$ =-0.000000001791821, $\lambda 8$ =0.000000000007781, $\lambda 9$ =-0.000000000000018, $\lambda 10$ =0.000000000000000

Table 3.4 shows the parameter(λ) values of various models.

Kolmogorov-Smirnov Test

Determination of the 3rd order model as a good fit over data is achieved by Kolmogorov-Smirnov goodness-test-using an Excel spreadsheet and MATLAB.

In Table 3.5, columns 1 and 2 are comprised of the data and their frequency. Column 3 represents the corresponding cumulative frequency values, and column 4 divides these values by the size of the sample 219, neglecting the 0 value from the sample size 220. Column 5 contains the values of the CDF acquired using MATLAB program. Lastly, column 6 is the variation between the values in column 5 and column 6. D_n holds the greatest value in column 6. The critical value of $D_{n,0.05}$ is obtained from Haldar & Mahadevan (2000). Considering that the value of D_n is less than $D_{n,0.05}$, we can conclude that the distribution data is a good fit with the 3rd model order of entropy distribution. The density function $f(y)$ for a random vari-

able y of the 3rd order is computed by applying the algorithm of maximum entropy formalism,

$$f(y) = exp(-6.73785094370 + 0.06528768351y - 0.00061791701y^2 + 0.00000145655y^3). \quad (3.32)$$

Table 3.5: K-S goodness-of-fit test of 3rd model order on 220 warehouse live load data

Data	Freq.	Cum freq.	$S_n(x)$	$F(X)$	Difference
0-20	5	5	0.0406504	0.053092	0.0124420
21-40	43	48	0.3902439	0.3227967	0.0674471
41-60	33	81	0.6585365	0.6896093	0.0310727
61-80	29	110	0.8943089	0.8956459	0.0013370
81-100	10	120	0.9756097	0.9737297	0.0018800
101-120	3	123	1	1.0090472	0.0090472
					D_n = 0.0029685
					$D_{n,219}$= 1.35810
					$D_{n,0.05}$ = 0.0062013

3.5 Summary

In this chapter, a new approach is developed to set up a distribution-free model of soil variables. The proposal includes a two-stage analysis based on maximum entropy formalism, and followed by Akaike's information criterion. The method produces an unbiased distribution-free model with an optimal order, which is then validated by Kolmogorov-Smirnov goodness-of-fit test. The uncertainties related to geotechnical variables are quantified systematically in the proposed approach. In addition, the process as men-

tioned above is validated by implementing it on three examples of data. The results generated by the analysis have certified that the procedure is reliable and efficient for large data values as well as a limited set of values.

Chapter 4

Soil Investigation

4.1 Introduction

The structure of the chapter is as follows: in Section 4.2, an insight to the Nipigon River landslide site history, geology and subsurface conditions is provided. In Section 4.3, the description of soil tests is provided, and the mechanism of the vane shear test is described. Also, the application of the vane shear test is performed to obtain the values of shear strength parameters of the slope in the Nipigon River area. Section 4.4 shows the results of the performed vane shear test. A summary is exhibited in the last Section 4.5.

4.2 History of the Nipigon Slope

The landslide in question occurred on the morning of April 23rd 1990, at the north area of the town of Nipigon, Ontario, Canada as in Figure 4.1. It involved almost 300,000 cu/m of soil extended almost 350 m inshore of the river with the maximum width of approximately 290 m (Dodds, Burak, & Eigenbrod, 1993). This landslide had an adverse impact on the environmental and economic condition of the region. River fluctuations of up to 1.2 meters were seen commonly, as stated by the locals.

The Trans Canada pipeline which operates under 7 MPa pressure, was displaced from its original position to about 8.3 meters in towards the river

and was left suspended without any support from the ground for up to 75 meters of its length. The fiber optic connections in the pipeline got shattered. Three major associations carried out their respective investigation in the following years after the landslide had taken place. Trow consulting engineers Ltd. was hired by the Trans Canada pipeline and the Ministry of Natural Resources to assess the cause, further risks, and recommendations for the operation of the Alexander hydroelectric power station, which is situated 8 km above the landslide area on the Nipigon River. Furthermore, investigations were carried out by Ontario Hydro as well as the department of civil engineering of Lakehead University.

Figure 4.1: Nipigon River landslide area (2018)

4.2.1 General Geology and Subsurface Conditions of Region

The land in this area mostly comprises of glaciolacustrine plain and pockets of sand silt in the delta. Figure 4.2 shows the location of the landslide site. The drainage conditions are relatively poor in the local relief. The human-made and natural slopes are susceptible to failure. The Arial photography report after the landslide revealed that the area had many bank failures even before the construction of the hydro dam in 1931 (Dodds, Burak, & Eigenbrod, 1993). The land is mostly wet with poor drainage conditions adding

instability to the banks of the region. The recent investigation in 2018 of the Nipigon slope by Lakehead university graduate civil engineering students, clearly depicts that the area is prone to small-scale slope failures as seen in Figure 4.7.

Figure 4.2: Location of landslide (source:Google maps)

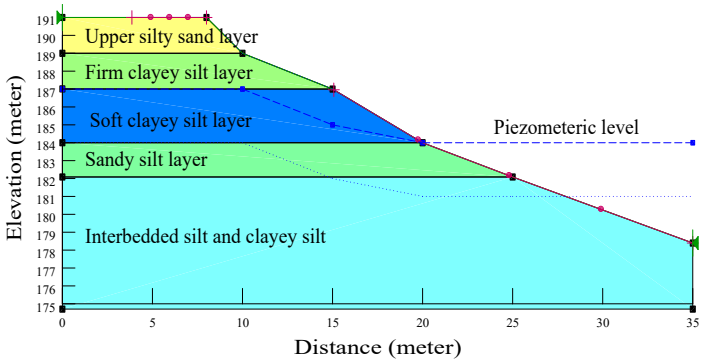

Figure 4.3: Subsurface conditions of the slope in the Nipigon River slope

The general soil stratum of different layers of the Nipigon slope consists of a silty sand layer on the top, beneath this layer is the clayey silt layer,

and the layer underneath the clayey silt layer is the silty sand and sandy silt layer. The soft silty layer and plastic clay /silt layers exist under the lower silt/sand layer. Figure 4.3 represents the subsurface conditions.

4.3 Soil Tests

The fine-grained soils commonly have drained and undrained shear strengths, which is related to the fact that pore water pressure is drained or not. The in-situ shear strength is obtained in undrained conditions because short term slope stability requires the undrained shear strength of soil. The laboratory technique's to compute undrained shear strength includes an unconfined compression test (UCT), direct shear test (DST), unconsolidated undrained test (UUT), and laboratory vane shear test (VSTL) . In the case of field investigation, the field vane shear test (VST) is the most frequently adopted method to get the undrained shear strength of soil (Jay, Nagaratnam, & Braja, 2016). The test produces a fast and robust computation approach for shear strength of undisturbed and remolded soil. Consequently, we use the vane shear field test in the present study

4.3.1 Vane Shear Field Test

The vane shear test is one of the most commonly adopted tests to analyze the undrained shear strength of the in-situ saturated cohesive soil (Jay, Nagaratnam, & Braja, 2016). The soils considered are weak and compressible, having the properties of soft to firm clayey soils. The soils that are cohesionless, such as sandy and gravel soil, are not able to maintain the undrained conditions, and cannot be tested with vane shear. The vane shear test is also not compatible with fibrous compost (Jay, Nagaratnam, & Braja, 2016). The vane shear test was invented in the twentieth century in Sweden.

A complete outline of the vane shear test is provided by Walker (1983). The vane shear test is a robust and time saving test, as compared to other tests, as it is easy and creates less disturbance of the soil while implementing the test on the soil. It is an in-situ test, carried out by advancing the test from the required depth to the base of the borehole. The over consolidation ratio of the soil can be computed by this test using the empirical rule. The vane shear test is more accurate than any other in-situ test to obtain the undrained shear strength of the clayey soil (Lunne & Robertson, 1997).

Procedure and Equipment of Vane Shear Test

The equipment of vane shear includes a solid pushing rod with two vertical vanes connected to the rod. A vane shear reading meter, which measures the value of the torque, is connected to the top of the rod. The test includes inserting the rod to the required depth and rotating the vane on its axis until the soil reaches a shear failure. The meter on the top of the vane records the reading. The depth of the test may vary from .5 to 1 meter or may be selected as required by the investigating engineer. Figure 4.4 shows parts of the vane shear equipment.

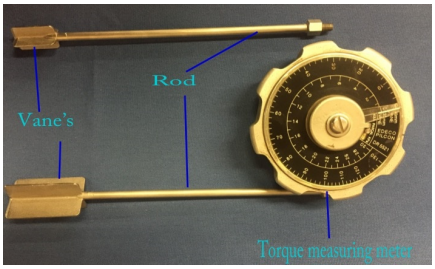

Figure 4.4: Vane shear equipment

The test procedure can be explained in following steps according to the ASTM D2573-08:

1. Place the vane shear equipment at the borehole. According to the required depth, the test can be carried out in the pre-drilled borehole or the rod can be inserted without drilling any hole before the test.
2. Push the vane slowly into the borehole or vane housing with a single thrust to the required depth.
3. After a few minutes apply torque at a rate of 0.1 deg/sec and record the maximum torque at the failure. Record the readings every 15 seconds.
4. Rotate the vane continuously 7 to 10 times and record the residual torque at the end.

Mechanism of the Vane Shear Test

As the test is carried out very rapidly at the site, an assumption is made, that the conditions are undrained and the shear stress at the failure is equal to the undrained shear strength, c_u (Jay, Nagaratnam, & Braja, 2016). Therefore, the maximum torque required to rotate the vane shear blades is as in Eq. (4.1).

$$T = M_{top} + M_{base} + M_{side}, \tag{4.1}$$

where T is the maximum torque, M_{top} is resisting moment at the top of the blades/cylinder, M_{base} represents resisting moment at the base of the blades/cylinder andM_{side} signifies the resisting moment at the sides of the blades/cylinder. Now taking moments about the shaft axis:

$$M_{side} = (\pi DH) \times c_u \times \frac{D}{2}, \tag{4.2}$$

and,

$$M_{top} = M_{base} = \int_0^{\frac{D}{2}(2\pi r dr)\times c_u \times r}, \tag{4.3}$$

where H is height of the vane, D represents width of the vane, c_u denotes the undrained shear strength, and r is radius of circular element of thickness (dr). Combining Eq.'s 4.1, 4.2 and 4.3, we get:

$$T = \left[(\pi DH) \times c_u \times \frac{D}{2}\right] + 2 \times \int_0^{\frac{D}{2}(2\pi r dr) \times c_u \times r}, \tag{4.4}$$

$$c_u = \frac{T}{\frac{7}{6}\pi D^3}, \tag{4.5}$$

$$c_u \quad or \quad S_u = T/(3.67D^3). \tag{4.6}$$

Eq. (4.6) gives the undrained shear strength with the help of maximum torque recorded. Consequently, the vane shear test device employed for field tests in the present study computes undrained shear strength (S_u) and works on the principle based on Eq. (4.6) as it is calibrated automatically to produce the actual value accordingly.

Test Corrections

Including the vane shear test, all other in-situ tests comprise some imperfections (Jay, Nagaratnam, & Braja, 2016). Bjerrum (1972) concluded that plasticity of soil has a huge influence on soil undrained shear strength obtained by the vane shear field test, and should be corrected before using the values for the design of embankment loading and slope stability. Bjerrum (1972) suggested that the undrained shear strength (c_u-field) from field the vane shear test needs to be multiplied by the correction factor μ to obtain the mobilized shear strength. The correction factor μ is related to the plasticity index (PI), and the relationship is shown in Figure 4.5. Figure 4.5 also represent the relationship based on the research done by Morris & Williams

(1996) and Chandler (1988).

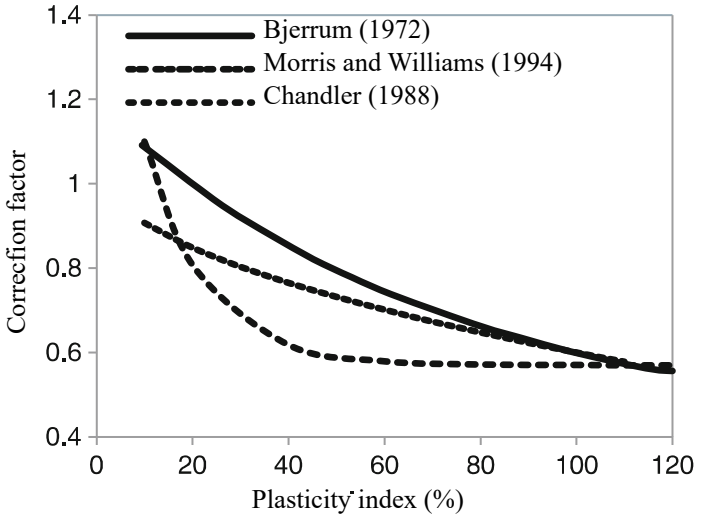

Figure 4.5: Field vane correction factor vs plasticity index (Jay, Nagaratnam, & Braja, 2016)

4.3.2 Nipigon Slope Field Investigation

The field work included drilling, soil sampling, and in-situ soil testing. The field investigation and testing was carried out by graduate masters of engineering students (Navjot Singh Kanwar, Sukhdeep Singh and Dhavan Joshi under supervisor Dr. Jian Deng) from Lakehead university civil engineering department. Various boreholes were drilled using vane shear. Site works included the vane shear test, and the collection of samples as shown in Figure 4.6. The vane shear tests were performed at various bore holes on the top 1 meter to 3 meter of the soil layer, generally in the firm clayey silt layer. The test was carried out at the Nipigon slope where the failure occurred in 1992, and the coordinates of the testing site are $49^0 4' 33" N\ 88^0 18' 34" W$. American Society for Testing and Materials (ASTM D2573-08) standards were followed to complete the vane shear test. The test was conducted at

various boreholes to get 123 values of undrained shear strength. Tools and the methodology for the test have been mentioned and explained in Section 4.3.1 and Section 4.3.2. The values of shear strength obtained from vane shear test are provided in Table 4.2.

Figure 4.6: Vane shear test on the Nipigon slope

Figure 4.7: Most recent small scale soil erosion at the Nipigon River banks (2018)

4.4 Results

Correction Factor

As undrained shear strength determined by the VST is influenced by effects of anisotropy and strain rate, hence, there is a need to correct the values obtained from the VST field test with a factor μ (Bjerrum, 1972). The laboratory test results by Lakehead university graduate students are given in Table 4.1. The average plasticity index value is taken as 20.5, from present investigation results. Therefore the resulting correction factor obtained is 0.95. The results of the vane shear test are provided in Table 4.2.

Table 4.1: Summary of laboratory testing

Sample	Liquid Limit	Plastic Limit	Plasticity Index	Liquidity Index	Moisture Content	Sand %	Silt %	Clay %
BH-l 1.5 - 2.1 m	45.5	24.7	20.8	0.33	31.5	11	71	18

Table 4.2: Corrected undrained shear strength (S_u, kPa) values from VST at the Nipigon river slope (123 values)

60.8	56.05	52.25	41.8	80.75	38.95	18.05	23.75	32.3	35.15
61.75	56.05	52.25	42.75	81.7	39.9	18.05	25.65	33.25	36.1
61.75	57	52.25	44.65	84.55	39.9	19	26.6	33.25	37.05
62.7	57	52.25	44.65	85.5	39.9	19	26.6	33.25	37.05
63.65	57	53.2	45.6	87.4	39.9	19	27.55	33.25	38
64.6	57	53.2	46.55	95	39.9	20.9	28.5	33.25	38
64.6	57.95	54.15	47.5	95	39.9	20.9	29.45	33.25	38
64.6	57.95	54.15	49.4	95	40.85	22.8	29.45	33.25	38
64.6	57.95	55.1	49.4	96.9	40.85	22.8	30.4	34.2	38
65.55	58.9	55.1	51.3	104.5	41.8	23.75	32.3	35.15	38
68.4	68.4	68.4	71.25	71.25	74.1	77.9	77.9	80.75	104.5
65.55	66.5	66.5	66.5	66.5	67.45	67.45	68.4	68.4	114
68.4									

4.5 Summary

The chapter above presents a concise summary of the soil tests, site specification of the Nipigon slope, application of the vane shear test, the procedure involved in the trial, and description of the data. Additionally, the comparison is made between the vane shear test, and other in-situ and laboratory test methods. The data collected from the procedure is further practiced in the next chapter to conduct reliability analysis on the soil variables of the Nipigon slope.

Chapter 5

Reliability Analysis of the Nipigon Slope

5.1 Introduction

This chapter presents an application of the proposed approach on the reliability analysis of the Nipigon slope. Firstly, in Section 5.2, the proposed maximum entropy formalism (MEF) and Akaike's information criteria (AIC) method will be applied to the soil data of the Nipigon slope obtained by the vane shear test to set up a distribution free model of soil variables.

Further, in Section 5.3 a first order reliability method is modified to be accompanied with the parallel response surface method and GEO-Slope procedure to carry out the reliability analysis. In Section 5.4, the probabilistic analysis is justified by implementing the proposed approach and comparing it with GEO-Slope based Monte Carlo simulation method. Section 5.5 provides the results of the reliability analysis, and sensitivity analysis. A summary is exhibited in the Section 5.6. The plan adopted in this chapter is presented in detail in Figure 5.1.

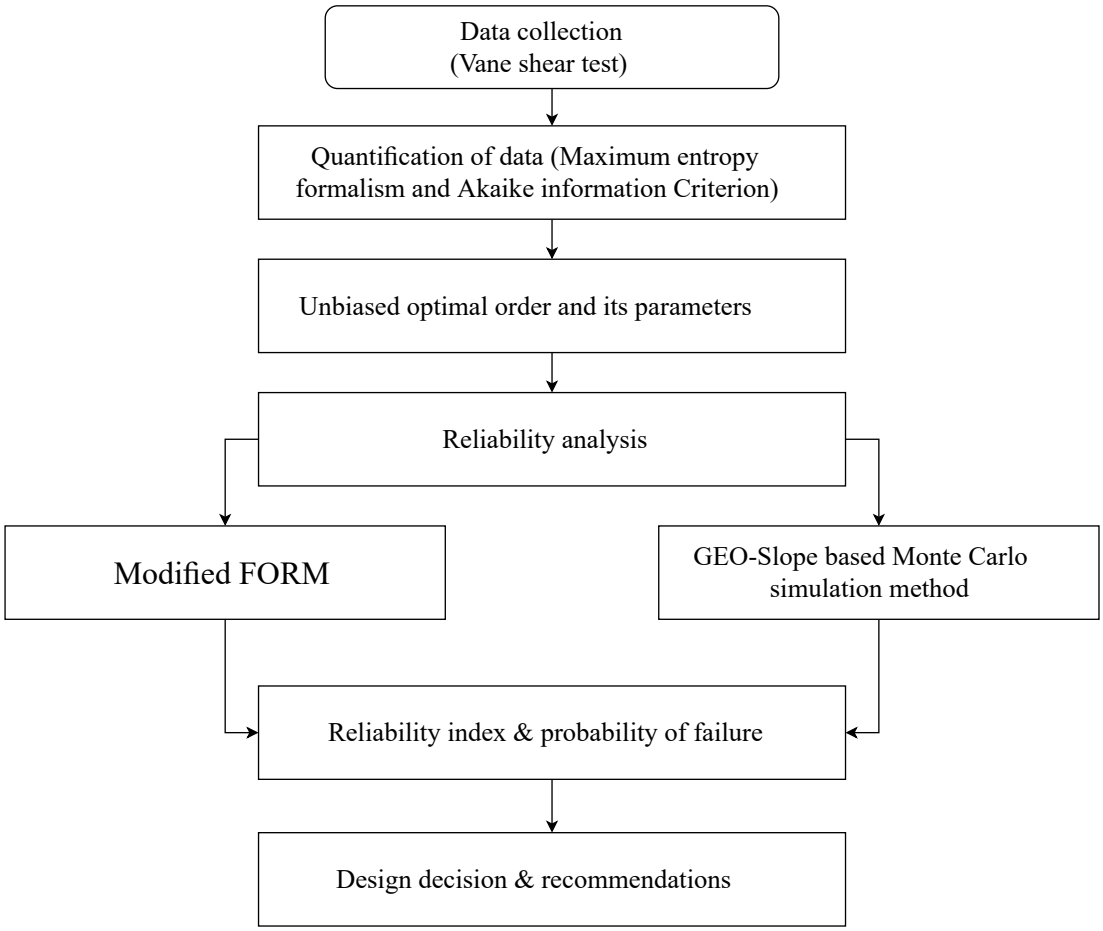

Figure 5.1: Flowchart for proposed reliability analysis method

5.2 Entropy-Based Probabilistic Distribution of the Nipigon Slope Soil Parameters

This Analysis is carried out on the sample of 123 data values of the Nipigon slope soil strata, given in Table 4.2. The vane shear test is performed at various boreholes on the Nipigon slope site to obtain the values of undrained

shear strength. Further, these measured values of undrained shear strength of the Nipigon slope are used to conduct analysis by the two-stage procedure of the maximum entropy formalism (MEF) and Akaike's information criterion (AIC). The results of maximum entropy with various models and their parameter values are presented below:

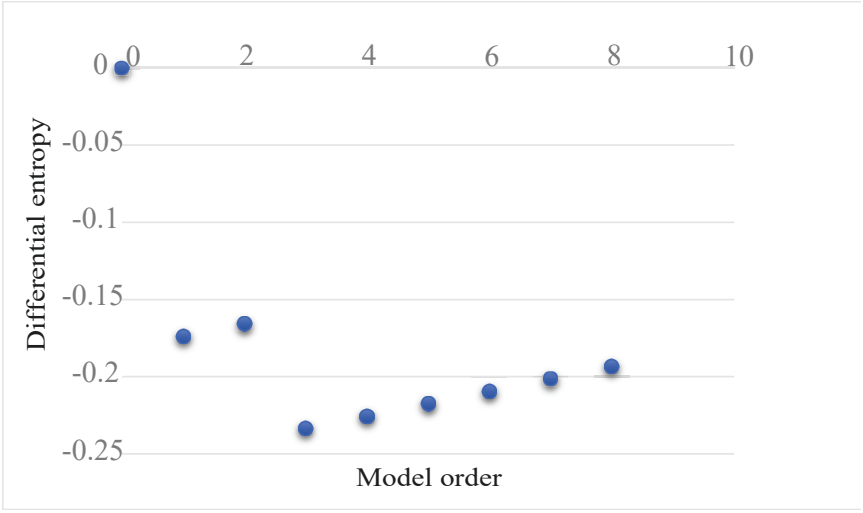

Figure 5.2: Differential entropy DH(K) of 123 sample of S_u of the Nipigon slope soil vane shear test data based on different model orders

Inspection of the Figure 5.2 shows the differential entropy for different model orders in transformed domain with $x_{min} = 0$ and $x_{max} = 150$. Figure 5.2 depicts that 3rd model order has the minimum value of differential entropy. Hence, the 3rd order model is an optimal order. The values of differential entropy for the 2nd and the 3rd order are very close, but the overall having lowest differential entropy value the 3rd order is considered an optimal.

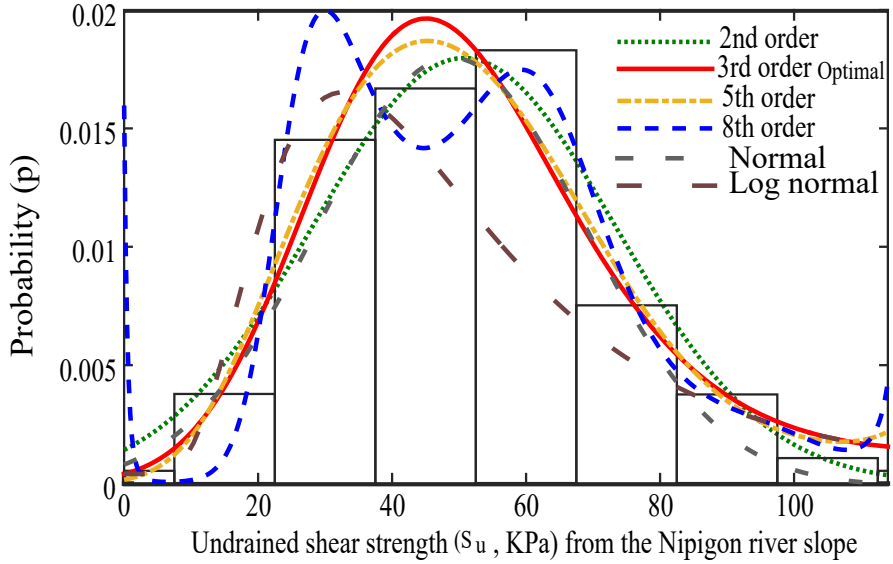

Figure 5.3: Data and density functions of sample of 123 S_u values from the vane shear test of the Nipigon slope soil

Figure 5.3 shows the histogram of the data of undrained shear strength for the Nipigon slope soil. Figure 5.3 consists of three superimposed density functions; the 2nd order model with the green dotted line, the 8th order model in the blue broken line and the 3rd order in bold red, which is optimal order.

Figure 5.3 depicts the fact that the 2nd order model fit nicely at some points than the optimal the 3rd order model, particularly between the range 0 to 25, and 60 to 100, but overall the 3rd model order fit the data better than the other orders. When an optimal 3rd order is compared with the 8th order, Figure 5.3 clearly shows that the 3rd order fit far more precisely than the 8th order. Also, entropy models are compared with classical normal and log-normal distributions in the Figure 5.3, it is inspected that both the distributions are not as good fit as 3rd model order. Therefore, it is reason-

able to choose the 3rd order rather than any other model order as an optimal order. Furthermore, a goodness-of-fit test can be utilized to validate that the selected 3rd optimal order is a good fit.

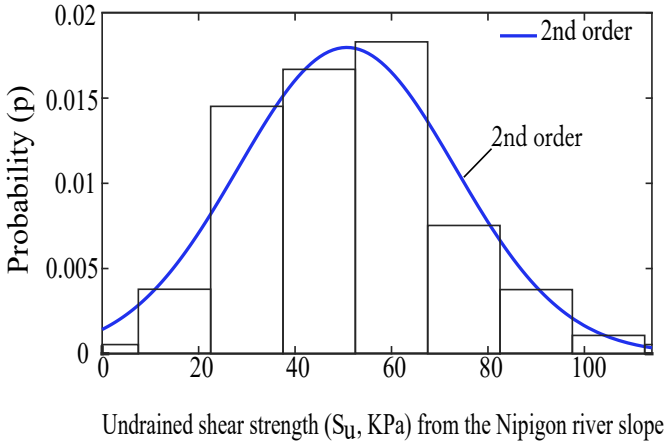

Figure 5.4: 2nd model order

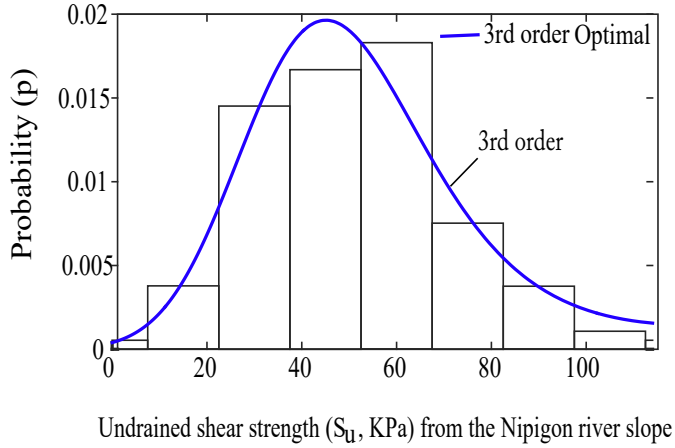

Figure 5.5: 3rd model order

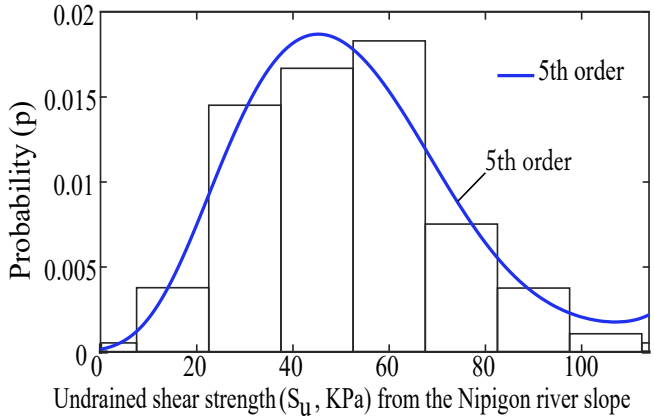

Figure 5.6: 5th model order

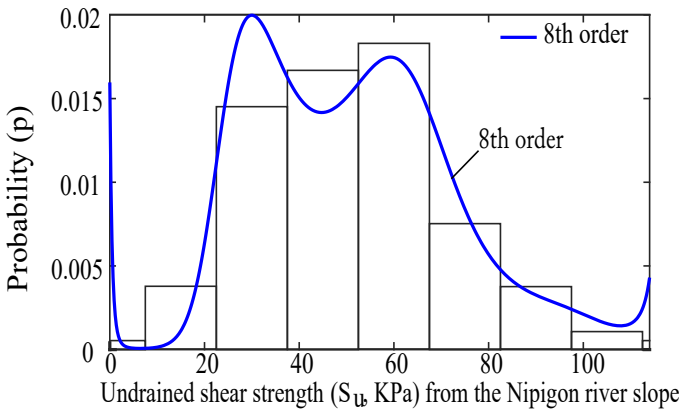

Figure 5.7: 8th model order

Figures 5.4, 5.5, 5.6 and 5.7 represents the 2nd, 3rd, 5th and 8th model order fitting over data respectively. Comparing the 2nd order and the 3rd order, it is evident that both orders are very much similar and fit the data very well. In between 0 to 15, the 2nd order is a better fit but in range 45 to 75 and 50 to 105, 3rd order fit more data. Furthermore, the 5th order is a good fit then the 8th order. Also, in Figure 5.8 4th and 3rd order are

compared, which shows that 3rd order is a better fit than 4th order. While looking at all the model orders fit, 3rd order is more accurate than other fits.

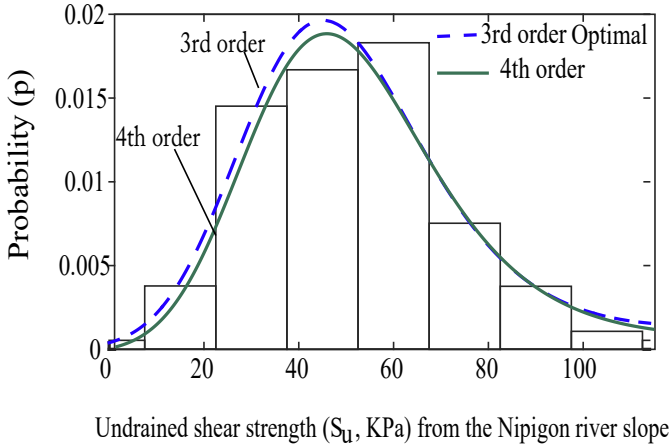

Figure 5.8: 4th model order

Table 5.1: Model parameters values of the Nipigon slope soil data

Model Order	Parameter (λ) Values
2nd	$\lambda 1$ =-6.554642216048960,$\lambda 2$ =0.099965883623882, $\lambda 3$ =-0.000985242747573
3rd(OPTIMAL)	$\lambda 1$ = -7.829086777427186, $\lambda 2$ =0.197665008964854, $\lambda 3$ =-0.003013909739996, $\lambda 4$ =0.000012150252884
4th	$\lambda 1$ =-7.950402872712516,$\lambda 2$ =0.211122965291184 , $\lambda 3$ =-0.003467708079757, $\lambda 4$ =0.000018018697990, $\lambda 5$ =-0.000000025433338
5th	$\lambda 1$ =-8.733759903153345, $\lambda 2$ =0.333151516620218, $\lambda 3$ =-0.009529318452856 , $\lambda 4$ =0.000146947108962, $\lambda 5$ =-0.000001246050034 , $\lambda 6$ =0.000000004218254
8th	$\lambda 1$ =-4.137304821442461, $\lambda 2$ =-2.085725113719108, $\lambda 3$ =0.268460678340851, $\lambda 4$ =-0.014002881239270, $\lambda 5$ =0.000385515541552, $\lambda 6$ =-0.000006078500094, $\lambda 7$ =0.000000055151349, $\lambda 8$ =-0.000000000267975, $\lambda 8$ =0.000000000000540

Table 5.1 shows the parameters (λ) of different model orders and opti-

mal 3rd model order. The 2nd model order has 3 (λ) parameters and 3rd optimal order has 4 (λ) values. Likewise, 5th order has 6 (λ) parameter values and 8th order has 9 (λ) parameter values. The optimal order 3 (λ) can be further used for designing purposes. These parameters can be used to estimate the distribution and density function. **Kolmogorov-Smirnov Test**

Table 5.2: K-S goodness-of-fit test of 3rd order on 123 S_u values of the Nipigon slope

Data	Freq.	Cum freq.	$S_n(x)$	$F(X)$	Difference
0-20	5	5	0.04065	0.05309	0.01244
21-40	43	48	0.39024	0.32279	0.067447
41-60	33	81	0.65853	0.68960	0.03107
61-80	29	110	0.89430	0.89564	0.00133
81-100	10	120	0.97560	0.97372	0.00188
101-120	3	123	1	1.0000	0.0000
					D_n = 0.01244
					$D_{n,46}$=1.3581
					$D_{n,0.05}$ = 0.12245

To determine that the 3rd model is ia a good fit over the data, Kolmogorov-Smirnov goodness-of-fit test is conducted using an Excel spreadsheet and MATLAB.

In Table 5.2 columns 1 and 2 consist of the data and its frequency. Column 3 represents the corresponding cumulative frequency values, and column 4 divides these values by the size of the sample 123. Column 5 represents the values of CDF obtained using MATLAB program. Finally, column 6 is the difference between the values in column 5 and column 6. D_n signifies the largest value in column 6. The critical value of $D_{n,0.05}$ is taken from Haldar & Mahadevan (2000). Since the value of D_n is less than

$D_{n,0.05}$, the 3rd model of entropy distribution is a good fit on data. The density function $f(y)$ for a random variable y of the 3rd order is computed by applying the algorithm of maximum entropy formalism,

$$f(y) = exp(-7.82908677742 + 0.19766500896y - 0.00301390973y^2 + 0.00001215025y^3). \quad (5.1)$$

5.3 Modified FORM for Entropy

The FORM method is modified to incorporate the non-normal parameters of entropy distribution obtained from maximum entropy formalism and Akaike's information criterion. The modification approach is carried out using a parameter equivalent normal transformation developed by Rackwitz and Fiessler in 1976 (Haldar & Mahadevan, 2000).

Rackwitz and Fiessler evaluated the parameters of equivalent normal distribution $\mu_{X_i}^N$ and $\sigma_{X_i}^N$, by following conditions and an algorithm. The cumulative density function and the probability density function of the original variables and equivalent normal variables should be identical at the checking point $(x_1^*, x_2^*, ..., x_n^*)$ on the failure surface.

$$\phi(\frac{x_i^* - \mu_{X_i}^N}{\sigma_{X_i}^N}) = F_{X_i}(x_i^*), \quad (5.2)$$

where $\phi()$ is CDF of standard normal variate and, $\mu_{X_i}^N$ and $\sigma_{X_i}^N$ are mean and standard deviation of an equivalent normal variable at the checking points. The $F_{X_i}(x_i^*)$ is the original CDF of nonnormal variable. Eq. (5.2) gives

$$\mu_{X_i}^N = x_i^* - \phi^{-1}[F_{X_i}(x_i^*)]\sigma_{X_i}^N, \quad (5.3)$$

furthermore, equating the PDF's of original the variable and equivalent non-

normal variable at the checking points yields

$$\frac{1}{\sigma_{X_i}^N}\phi(\frac{x_i^* - \mu_{X_i}^N}{\sigma_{X_i}^N}) = f_{X_i}(x_i^*), \tag{5.4}$$

where $\phi()$ and $f_{X_i}(x_i^*)$ are the PDF's of the equivalent standard normal and the original nonnormal variables. Eq. (5.4) yields

$$\sigma_{X_i}^N = \frac{\phi(\phi^{-1}[F_{X_i}(x_i^*)])}{f_{X_i}(x_i^*)}. \tag{5.5}$$

Hence, equivalent standard normal variables are determined by these equations and can further be used in FORM to compute reliability index β_{HL}. The steps for the FORM method to evaluate the reliability or safety index are described as below. (Haldar & Mahadevan, 2000).

1. Define the appropriate limit state equation (obtained from response surface method).
2. Then, assume an initial value of the safety index β. Any value can be assumed, that allows β to converge quickly.
3. Next step is to assume the initial values of the design point x^*, i= 1,2, ..., n. The initial design point can be considered to be at the mean and standard deviation values of the random variables.
4. Estimate the mean and standard deviation at the design point of the equivalent normal distribution for nonnormal variables.
5. Calculate partial derivatives $(\partial g \,/\partial X_i)^*$ computed at the design point x^*.
6. Measure the direction cosines α at the design point as:

$$\alpha_{X_i} = \frac{(\frac{\partial g}{\partial X_i})^* \sigma_{X_i}^N}{\sqrt{\sum_{i=1}^n (\frac{\partial g}{\partial X_i}\sigma_{X_i}^N)^{2^*}}}. \tag{5.6}$$

7. Calculate the new values of checking points x_i^* as

$$x_i^* = \mu_{X_i}^N - \alpha_i \beta \sigma_{X_i}^N. \tag{5.7}$$

   If required repeat steps 4 to 7 again until the direction cosines α_i converges to the tolerance level of 0.005. When the direction cosines converge new checking point can be computed keeping β unknown.
8. Keeping the condition that limit state equation must be satisfied at new checking points the updated value of β can be estimated.
9. Repeat steps 2 to 8 until β converges to the tolerance level of 0.001

The algorithm converges quickly in a few cycles, depending upon how linear the limit state equation is. A computer program in MATLAB is constructed for the analysis to carry out the computations.

The FORM method is require to define the performance function to carry out reliability analysis using above algorithm described above. The critical problem that arises while solving derivatives of the performance function is its non-linearity. Hence, an approach is developed in Section 5.3.1 to compute linear performance function using the response surface method.

5.3.1 GEO-Slope and Response Surface Method for Performance Function

The random variables are chosen after careful considerations of the parameters in the problem under study. The uncertainties involved with the parameters were examined using MEF and AIC. Furthermore, an experimental slope model is set up in GEO-Slope 2007 version. For each set of input variables required, the factor of safety is generated using the Morgenstern Price method in the GEO-Slope. The corresponding outcome of the

factor of safety for various input variables is used to develop the linear response surface models, and then eventually, these models develops the limit state function. The first order reliability method is enhanced and modified to compute the reliability index using the MATLAB function with the performance function as a constraint. The probability of failure is computed after calculating the value of the reliability index.

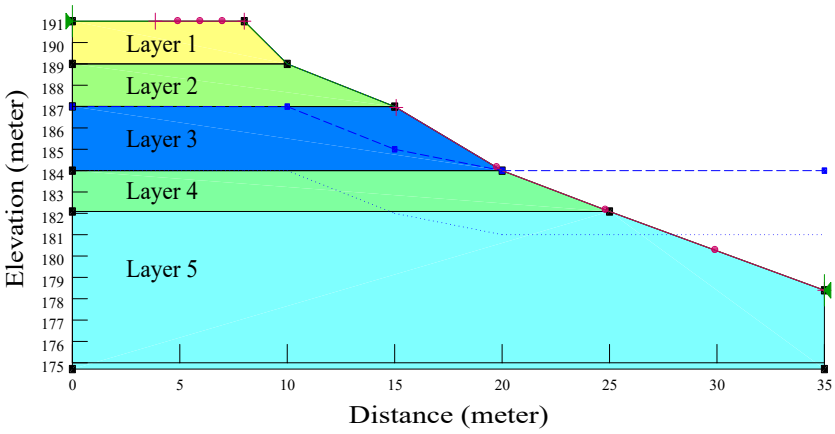

Figure 5.9: GEO-Slope defined model of the Nipigon slope

The GEO-Slope software is considered under different conditions to carry out slope stability of the Nipigon slope. Initially, the geometry of the slope as shown in Figure 5.9 is created using SLOPE/W analysis. As per the slope conditions, the entry and exit location are assigned as left to right. Then the shear strength parameters: material properties for the different layer of the slope, and piezometric line, are defined and rectified according to the five different layers or zones of slope used in the analysis. The analysis is carried out using various limit equilibrium methods, i.e., Bishop, Janbu, ordinary method of slice and Morgenstern Price method accordingly. Finally, a minimum safety factor is calculated for the different mean values of the shear strength parameters assigned to materials, in combination with

response surface method.

Response Surface Method Optimized Using GEO-Slope

The response surface method was developed by Box and Wilson in 1951 (Draper, 1992). It is the collection of statistical techniques that optimize the process through an empirical model building. It works on the methodology of practicing the adjustment of the predictor variable to take the response in the desired optimum direction using iterations. The method is more straightforward than non-linear techniques as it uses quadratic response surface models. The response surface method includes the response surface analysis as well as the design of the experiments. Response surface models are multivariate polynomial models that develop during the design of experiments. These are then used to predict a set of design variables that optimize a response.

The available data is eliminated, and quality is enhanced by manipulating the data generation method. Series of runs of changes are made in the input to get the causes of failure in the output response. The main aim of the design experiments is to collect data without any complications and to provide ample information to determine the parameters correctly. Response surface analysis is based on the process of data interpolation to predict all type of correlations between the variables and objectives. First order model is enough for the flat data surface. Eq. (5.8) below represents a simple model of a response y in an experiment with two controlled factors (Subramaniam, 2011):

$$y = \beta_1 + \beta_1 x_1 + \beta_2 x_2 + \beta_{12} x_1 x_2 + \epsilon, \tag{5.8}$$

where x_n are random variables and β represents their correlation coefficients.

Factorial Design

In factorial experiment, the design variables are varied together at one time. The joint effect of the variables on the response variable is investigated using factorial designs (Subramaniam, 2011). One of the important case of the factorial design is two level factors, in which each k factors of interest have only two levels. The design has 2^k experimental trials and are known as factorial designs. This is helpful in developing the response surface designs.

The performance function is based on soil variables of slope is an explicit function, its converted into implicit function to incorporate it into modified first order reliability method for reliability analysis. Hence, response surface factorial design method regression analysis is used to generate linear implicit performance function. Uncertainty associated with soil variability are taken into account, and the shear strength parameters are considered as random variables. Table 5.3 shows the variables of different layers of soil used in the analysis.

Table 5.3: Mean(μ) and Coefficient of variation of soil variables

Layer	Unit Wt. (γ) (kN/m^3)	Undrained Shear Strength S_u (kPa)	Angle Of Friction (ϕ°)
Upper silty sand layer(Layer 1)	17.6		30
Firm clayey silt(Layer 2)	19	51.277	
Soft clay silt(Layer 3)	18.2	25	
Sandy silt(Layer 4)	17.6		30
Inter-bedded silt and clayey silt(Layer 5)	19.5	30	
COV	0.3	0.3	0.3

The regression analysis is performed on the least square approach. Each point in the design set is quantified using a lower limit ($\mu + 1.65\sigma$) and an

upper limit ($\mu - 1.65\sigma$) of each variable of parameter using Geo-Slope limit equilibrium deterministic method analysis.

Full Factorial Design Matlab code for the design of experiments (Subramaniam, 2011):

»dFF2 =ff2n(n)

dFF2 is R-by-C, where R represents the number of treatment in the full factorial design. As the variables used in this analysis are 5. Hence, the Matlab code used is:

»dFF2 =ff2n(5)

which gives the output in Table 7.1.

Table 7.2 reveals the results of the FOS of the Nipigon slopes corresponding to thirty-two sample points RSM analysis using GEO-Slope 2007. Next, the regression analysis is carried out using an Excel solver using the data in Table 7.2. Figure 7.1 & 7.2 shows the Excel sheet for RSM regression analysis. The preliminary analysis results confirm that the slip surface passes through layer 2 due to variability in layer 1 and layer 3.

Regression analysis gives out a linear response surface performance model as:

$$F = -0.31756666 + 9.55063E-05 * \phi_{(layer1)} + 0.008294003 * S_{u(layer2)} + 0.012097125 * S_{u(layer3)} + 0.006454125 * S_{u(layer4)} + 0.018008944 * \phi_{(layer5)}, \tag{5.9}$$

where ϕ, S_u are random variables respectively. F signifies the factor of safety. The limit state function in probabilistic slope stability is well defined

by Chowdhury et al. (2009) as:

$$F(x_1, x_2, ..., x_n) - 1 = g(x), \tag{5.10}$$

where $g(x)$ id the limit state function.

5.4 Entropy Based Reliability Analysis of Nipigon Slope

Modified FORM

The response surface performance function obtained from response surface regression analysis is incorporated into the first order reliability method to conduct a reliability analysis. A MATLAB program is developed for FORM to compute the reliability index and probability of failure of the slope. Covariance values of 0.1, 0.2, 0.3 are respectively used as three different cases for analysis. The probability of failure of the slope is given by:

$$p_f = \varphi(-\beta), \tag{5.11}$$

where p_f signifies probability of failure, and β denotes reliability index.

Monte Carlo Simulation of Slope Stability

Monte Carlo simulations with 300,000 iterations were performed using the software GEO-Slope 2007 on the Nipigon slope to compare it with the FORM method. The soil variables mean and standard deviations values are given in Table 5.4.

The initial step in the Monte Carlo simulation method is to identify the deterministic model to be adopted, and the next step is to determine the number of random variables used in the analysis. Further, the distribution

of all the random variables is chosen to initiate the trial process to compute the probability density function based on the deterministic model. Every trial includes a new random value from the distribution function to carry out the calculation. In the present analysis, precisely 300,000 tests are carried out by creating multiple passes using GEO-Slope 2007 software to obtain the results for each trial. Finally, the Monte Carlo simulation results in the probability density function of the factor of safety. The analysis done by the Monte Carlo simulation is conducted using four different deterministic methods which are Ordinary, Janbu, Bishops and Morgenstern-Price.

Table 5.4: Mean and standard deviation (SD) of soil variables for Monte Carlo simulation

Layer	Unit Weight (γ) (kN/m^3)	Undrained Shear Strength S_u (kPa) (Mean)	Undrained Shear Strength S_u (kPa) (SD)	Angle Of Friction (ϕ°) (Mean)	Angle Of Friction (ϕ°) (SD)
Upper silty sand layer(Layer 1)	17.6			30	9
Firm clayey silt(Layer 2)	19	51.277	15.3831		
Soft clayey silt(Layer 3)	18.2	25	7.5		
Sandy silt silt(Layer 4)	17.6			30	9
Inter-bedded silt and clayey silt(Layer 5)	19.5	30	9		

Sensitivity Analysis

In order to examine the influences of cross-correlation between the shear strength parameters of soil in the system reliability of slope stability analysis, a sensitivity examination is conducted by alternating the values of undrained shear strength (S_u) and angle of friction (ϕ) described in Table 5.5. the values of frictional angle and other layers undrained shear strength are assumed from Dodds et al. (1993), as stated in earlier chapters. Sensitivity analysis is carried out using in GEO-Slope software.

Table 5.5: Variation in values assumed for sensitivity analysis

Layer	Unit Weight (γ) (kN/m^3)	Undrained Shear Strength Su (kPa)	Angle Of Friction (ϕ°)
Upper silty sand layer(Layer 1)	17.6		20-40
Firm clayey silt(Layer 2)	19	41.277-61.277	
Soft clayey silt(Layer 3)	18.2	15-35	
Sandy silt silt(Layer 4)	17.6		20-40
Inter-bedded silt and clayey silt(Layer 5)	19.5	12-32	

5.5 Results

Table 5.6 exhibits changes in the values of the reliability index and the probability of failure with covariance values of 0.1, 0.2, and 0.3. The results represent that the reliability index decreases with increase in covariance. Whereas, the probability of failure increases with covariance increase.

Table 5.6: Probability of failure and reliability index with different covariance values

FORM	Reliability Index(β)	Probability Of Failure (p_f)
Cov = 0.1	0.8148	0.2076
Cov = 0.2	0.4070	0.3420
Cov = 0.3	0.2725	0.3926

According to the chart in Figure 5.10, it is evident that the analysis of the Nipigon slope results in extremely hazardous in all three cases. The factor of safety in all cases is going to be more than 1, but eventually the slope will fail. Therefore, the examination is a valid reason to demonstrate the significance of reliability analysis.

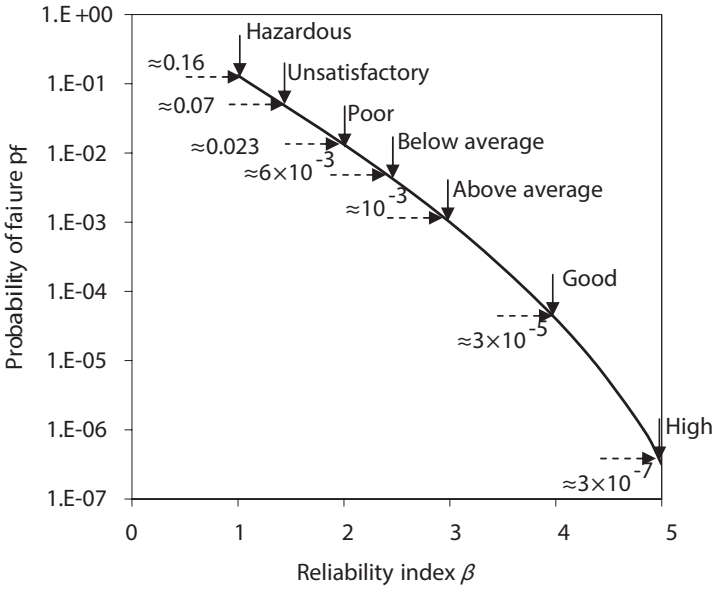

Figure 5.10: Relationship between reliability index (β) and probability of failure (p_f) USACE (1997) (Babu & Srivastava, 2010)

Table 5.7 summarizes factor of safety values computed by the Monte Carlo simulation for various deterministic methods. In the analysis results, the factor of safety differs for all four approaches which is mainly due to uncertainties in the variables. Morgenstern-Price method is more efficient as it considers both force and moment equilibrium, resulting in fewer uncertainties. Accordingly, the factor of safety obtained from Morgenstern-Price is considered for further analysis. Overall, the values of FOS for all four methods are nearly the same and indicates that the slope is in the hazardous stage of failure.

Table 5.7: Factor of safety for various deterministic methods using Monte Carlo simulation

Method (MCS)	Factot Of Safety
Ordinary	0.891
Bishop	0.967
Janbu	0.949
Morgentern-Price	1.005

Table 5.8: Results of probabilistic analysis using Monte Carlo simulation

Mean FOS	Min FOS	Max FOS	Reliability Index	Probability of Failure	Standard Deviation
1.0939	0.13235	1.9777	0.452	0.330781	0.208

Table 5.8 exhibits the results of the probabilistic analysis using the Monte Carlo simulation. The results infer that the value of the reliability index symbolizes that the slope is critically unstable. The equivalent factor of safety (FOS) behavior is described in Figure 5.11. Accordingly, allowable risk criterion can be taken into account to attain an objective target for the designing purpose.

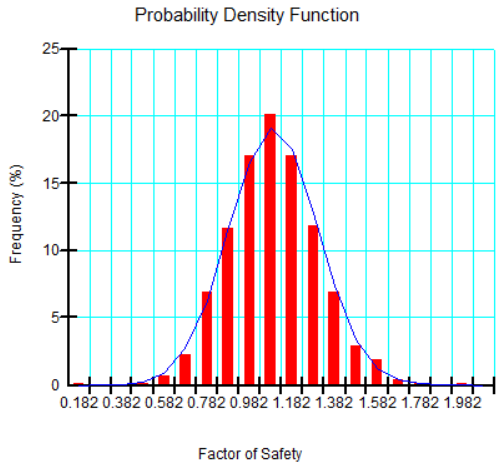

Figure 5.11: Histogram plot and distribution fit of factor of safety (FOS) for 300,000 realizations

Comparing the results of modified FORM and MCS, it is evident that the failure probabilities obtained have very little difference for covariance 0.3. The results of p_f by FORM is approximately 39% and by MCS is approximately 33%, the difference is due to the fact that modified FORM is able to consider the correlations between the soil variables explicitly, thereby producing more accurate results than Monte Carlo simulation. As the difference between the results by modified FORM and MCS are not large, it proves that the adopted method is very precise and incorporates the uncertainties comprehensively, along with the maximum entropy formalism approach.

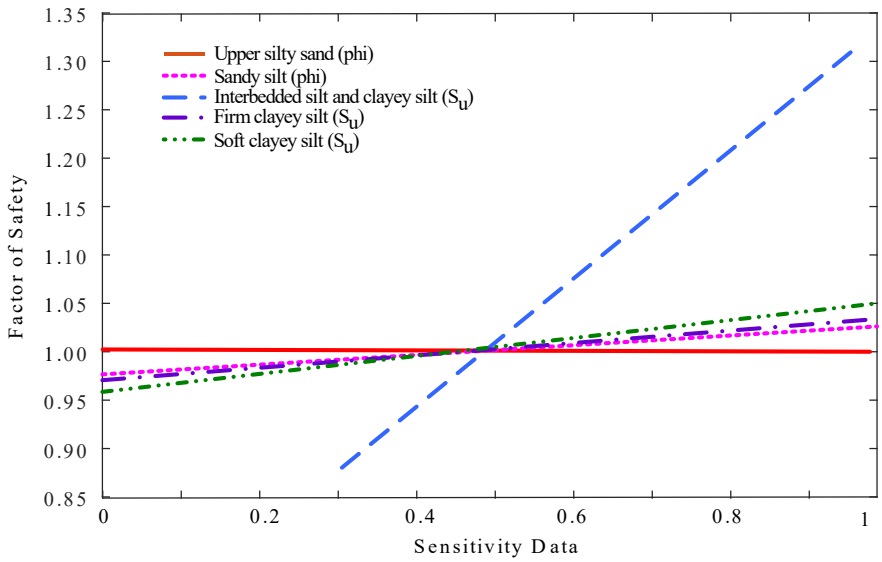

Figure 5.12: Variation in factor of safety with respect to given range of parameters

The results of sensitivity analysis are depicted in Figure 5.12. The solid-red line in Figure 5.12 reveals how the factor of safety changes with

the variation of $(20^\circ - 40^\circ)$ in unit friction angle (ϕ) of the upper silty sand layer. The uneven-purple line illustrates the contrast in the factor of safety over the range of 41.277-61.277 (kPa) that is specified for change in undrained shear strength for the firm clayey silt layer. The dotted-pink line reveals the difference in the factor of safety for the range $(20^\circ - 40^\circ)$ of friction angle defined for the sandy silt layer. The broken-blue line shows the variation in the factor of safety for undrained shear strength values between 12-32 (kPa) for the inter-bedded silt and clayey silt layer. Also, the dashed-green line describes the distinction in factor safety with the difference of 15-35 (kPa) in undrained shear strength (degree) for the soft clayey silt layer. In this graph, the sensitivity range is normalized between 0 to 1. The curves cross over 0.5 which denotes the static scale. This scale introduces how the factor of safety switches within the range defined in the dispersion of data.

Furthermore, the upper silty sand layer difference in friction angle does not influence the factor of safety. The firm clayey silt layer, the sandy silt layer, and the soft clayey silt layer yields about a decent decrease of 0.5 for a value lower than the actual value of 51.277 (kPa) and 25 (kPa) for S_u and 30° for (ϕ), used for probabilistic analysis and an adequate gain of 0.5 for real analysis value. The change in undrained shear strength values between 12-32 (kPa) as compared to the standard value of 30 in the probabilistic analysis for the inter-bedded silt seems to impact the factor of safety largely, and hence is the most significant factor for the slope failure. The decrease in the range of undrained shear strength for inter-bedded silt results in lowering the factor of safety required, by 0.10. Moreover, increase in the undrained shear strength, tends to enhance the factor of safety by almost 0.35.

5.6 Summary

In this chapter, an improved probabilistic procedure applying the modified first order reliability method (FORM) based on entropy generated non-normal parameters is proposed to implement a conceptually more rationalized method to consider the uncertainties to conduct slope stability analysis on the Nipigon slope.

Initially, site investigation to get undrained shear strength parameters of the Nipigon slope site using the vane shear test is illustrated. The soil variables obtained from the vane shear test and assumed from previous laboratory reports by Trow and Lakehead University are characterized using the maximum entropy formalism and Akaike's information criterion. The proposed method efficiently quantified the uncertainties associated with the soil parameters and generates the most unbiased and optimal order of the Nipigon slope soil data.

Further, an entropy-based modified (FORM) first order reliability method probabilistic approach was developed to account for non-normal parameters generated by maximum entropy probability density function. The performance function is produced utilizing the response surface method and GEO-Slope software. Above procedure is carried out by performing regression analysis on the factor safety obtained by correlating the soil parameters of the different layer in GEO-Slope software Slope/W analysis.

Later, the explicit performance function is incorporated in a modified MATLAB first order reliability method to compute the reliability index (β) and probability of failure (p_f). The proposed probabilistic approach seems to incorporate the uncertainties efficiently and dynamically. The results appear to signify that the Nipigon slope is hazardous and critically failure.

Additionally, the analysis is accompanied by a comparative study of Monte Carlo simulation method using the GEO-Slope software to perform

reliability analysis. The results produced by Monte Carlo simulations resembled the modified first order reliability method which validates that the introduced approach is more efficient and robust.

Chapter 6

Reliability Based Design of Slopes

6.1 Introduction

The study in previous chapters has revealed that stabilization of unstable slopes is a significant geotechnical concern that must be addressed to ensure the safety of structures. In slope engineering design, a traditional deterministic design approach has been adopted to lessen the cost and enhance quality rationally. The traditional deterministic design is inadequate to distinguish among the inherent variability and the internal scattering of the geotechnical variables, as these measures of central tendency are selected based on field tests and engineering systems (Phoon & Kulhawy, 1999). Nevertheless, the presence of uncertainties in soil properties such as spatial variability or modelling variability demands more rational and robust approach of a reliability-based design optimization (RBDO) model for reliable and cost-efficient designs.

Inside the RBDO model, the mean values generated from the systematic reliability analysis are adopted as design variables, and the cost is optimized based on probabilistic constraints employing nonlinear mathematical model programming (Tu, Choi, & Park, 1999). Therefore, the outcome of RBDO is a propitious design as well as extremely reliable and cost-effective design.

The composition of the chapter is as follows. In Section 6.2, an insight is provided to a reliability based design approach of pile slope systems.

Section 6.3 exhibits the entropy-based reliability analysis of a pile reinforced slope, with a description on pile design and the procedure of design is discussed as well. Section 6.4 presents the results of a reliability based design of the slope in the Nipigon River area, ans also confers the conclusion drawn from the design procedure application. In the end, Section 6.6 summarizes the whole chapter.

6.2 Reliability-Based Design for Piles Slope System

The reliability-based designs require a series of levels associated to determine geotechnical variables properties and field components that are accountable for influencing the probability of failure of geotechnical structures. Aforementioned field has attained a vast area of interest within the prior few years, which may be due to advancements in enhanced computational modeling for sophisticated statistical analysis procedures. The proposed study works on the same principles that were demonstrated in previous chapters.

Piles are long, slender components that may be manufactured of steel, concrete, timber, or polymer used for structural foundations. Piles lately have been applied to receive tensile and lateral loads, to diminish shaft load, and to lessen settlement of mat foundation. Additionally, piles are adopted for improving the stability of slopes possessing loose and expansive soils. The slope stabilization using piles has been successfully used by various researchers (Shin et al., 2006; Kao, 1985; Hassiotis et al., 1997; Poulos, 1995)

The soil properties, such as undrained shear strength (S_u), unit weight (γ), the angle of friction (ϕ) and pile variables, such as shaft resistance, the

spacing between piles (S) and depth of the pile (H) influence the uncertainties of slope system. The existing chapter deals with the treatment of pile reinforced slope uncertainties. Pile associated variables are treated as certain, while the soil variables are regarded as uncertain in the reliability-based analysis method. The characterization of soil variables is aided by the proposed maximum entropy and Akaike's information criterion methodology, followed by direct GEO-Slope-based Monte Carlo simulation for assessing reliability analysis.

6.3 Entropy Based Stability Analysis of Piles Slope System

As analyzed in the preceding chapters, MEF and AIC can be employed to quantify and characterize the soil shear strength parameters. Once the density function is acquired from the aforementioned probabilistic approach, the output is incorporated into GEO-Slope-based Monte Carlo simulation for evaluating reliability analysis.

MEF and AIC generates the an unbiased, and optimal order of probability assignments accounting for maximum uncertainties associated with the soil properties. The probability of failure for pile slope system is estimated using GEO-Slope-based Monte Carlo simulation. In this investigation, the probabilistic version of GEO-Slope 2007 computer software Slope/W is adopted for the reliability analysis of pile reinforced slope. The probability of failure of pile slope is calculated based on the Eq's. 6.1, and 6.2.

$$P_f = E(I[x]) = \frac{1}{N}\sum_{i=1}^{N} I[FS < 1], \tag{6.1}$$

where P_f is computed probability of failure for a pile drilled slope system,

$I[FS < 1]$ is the indicator function and N is the sample number.

$$\beta = 1 - \phi(P_f). \tag{6.2}$$

where β represents a reliability index and ϕ signifies the CDF . When the probability of failure is greater than 0.5, β can be negative.

Maximum Entropy and Akaike's Information Criterion for Soil Variables Modelling

The shear strength parameters are collected from field tests using the vane shear test. The values obtained are quantified using the proposed MEF and AIC method. The uncertainties are incorporated automatically in the approach systematically.

GEO-Slope-Based Monte Carlo Method

The computational algorithms of the GEO-Slope-based Monte Carlo method after incorporating entropy variables are illustrated below and represented in Figure 6.1.

- Specify the slope and pile geometry.
- Specify the materials and soil variables values in the key in section.
- Specify the pile location and combination.
- Perform Monte Carlo simulations using Morgenstern price limit state equilibrium method.
- Solve the analysis to obtain the factor of safety and the compute reliability index β using optimization approach.

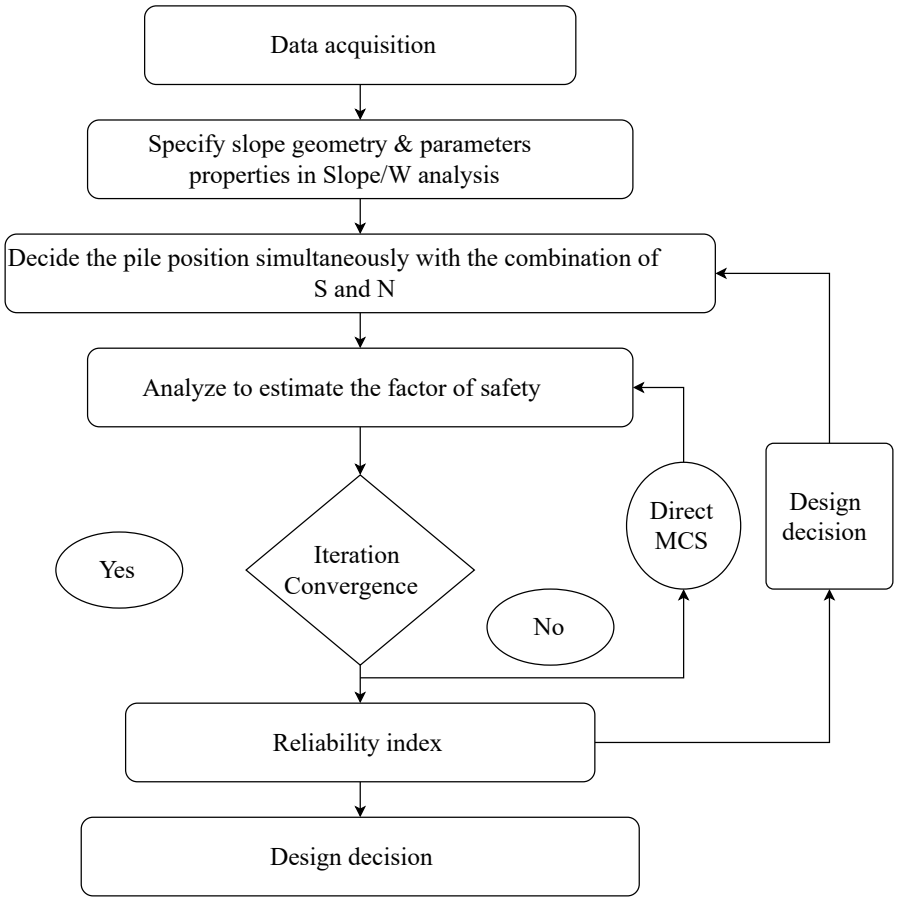

Figure 6.1: Flowchart representing the probabilistic pile slope design procedure using Reliability Based Design Optimization

6.3.1 Reliability Based Design of the Nipigon Slope

RBD application on the slope in the Nipigon River area illustrates the efficiency and working of the RBD method. The general design procedure adopted follows closely which is illustrated by L. Li & Liang (2013). As the findings from the probabilistic slope stability analysis by the proposed method in chapter 5 state, the slope in the Nipigon River area is a failure

slope, hence, pile reinforcement is designed to the slope to enhance its stability. Therefore, the slope is reinforced with piles. Continuous-flight auger piles are adopted. The specifications of the pile are given below in Table 6.3 (Salgado, 2006).

The GEO-Slope 2007 software is adapted to carry out the analysis. The slope model displayed in Figure 6.2 consists of five soil layers with soil properties for every layer reviewed in Table 5.4, in which the soil variables for the five soil layers follow a similar independent distribution. The critical slip surface is defined in the slope geometry. The piezometric line is established at about 186 meters as in the previous probabilistic analysis of the slope in the Nipigon River area. Effective stress approach is being used in the analysis.

6.3.2 Pile Design

The ratio of ultimate unit base resistance to limit unit shaft resistance in clay is less than that of the sand. Which in turn makes shaft resistance in clay more critical than in sand. Shaft capacity of piles can be computed either using total stress analysis or by useful stress analysis. In the present study, the total stress analysis method or α method is adapted to calculate the shaft resistance (shear force) of pile. The Eq. (6.3) calculates the limit unit shaft resistance.

$$q_{sL} = \alpha S_u, \tag{6.3}$$

where q_{sL} is limit unit shaft resistance, α represents the coefficient of resistance, and S_u signifies the undrained shear strength of clay (Salgado, 2006). In this case, non-displacement piles known as Continuous Flight Auger piles (CFA) are exercised because of their simplicity and feasibility.

Unit base and shaft resistance of CFA pile in clay design is adopted from Salgado (2006), and calculations are presented in Table 6.1.

Table 6.1: Calculations of CFA pile in clay design by O'Neill (1999)

Limit unit shaft resistance q_{sL}	Net ultimate unit base resistance $q_{b10\%}$
$q_{sL} = \alpha S_u$, $\alpha = 0.55$	$8S_u$, if 50 $S_u \leq$ 100 kPa

The ultimate shaft resistance can now be computed by Eq. (6.4).

$$Q_{ult} = q_{sL} + q_{b10\%}. \tag{6.4}$$

where Q_{ult} is the ultimate shaft resistance. q_{sL} represents limit unit shaft resistance and $q_{b10\%}$ signifies net ultimate unit base resistance. Therefore, using Table 6.1 the values obtained for CFA pile design are summarized in Table 6.2.

Table 6.2: Properties of CFA piles used in GEO-Slope analysis

Undrained shear strength S_u	Limit unit shaft resistance q_{sL}	Net ultimate unit base resistance $q_{b10\%}$	Ultimate shaft resistance or shear force $q_{b10\%}$
51.277 kPa	28.20	410.216	438.416 kN

Table 6.3: Soil properties of the Nipigon slope

Layer	Unit Weight (γ)(kN/m^3)	Undrained Shear Strength S_u (kPa) Mean	Undrained Shear Strength S_u (kPa) SD	Angle Of Friction (ϕ^0) Mean	Angle Of Friction (ϕ^0) SD
Upper silty sand layer(Layer 1)	17.6			30	9
Firm clayey silt(Layer 2)	19	51.277	15.3831		
Soft clayey silt(Layer 3)	18.2	25	7.5		
Sandy silt silt(Layer 4)	17.6			30	9
Inter-bedded silt and clayey silt(Layer 5)	19.5	30	9		

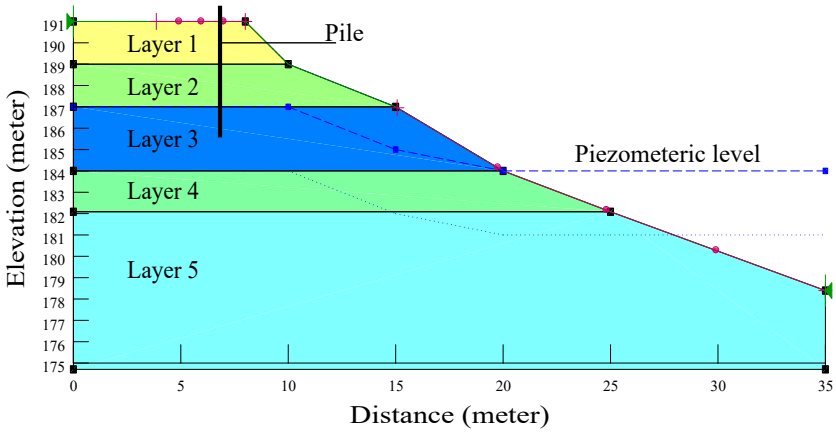

Figure 6.2: Slope geometry for pile slope system design of the slope in the Nipigon River area

6.3.3 Design Procedure

- **Step 1.** Obtain and specify the data required for the slope model, soil variables of the slope, and piezometric level. Figure 6.2 represents the model of the slope. The variables of the slope and pile are depicted in Table 6.3

- **Step 2.** Select different locations of the pile to be applied. Reasonable positions for a pile are between 191m to 183m.

- **Step 3. Case 1.** Initially, different pairs of clear spacing (S) and the different number (quantity) of pile (N) combination within the allowable range is selected. Combination mentioned above depends upon the site access and availability of construction resources. In this study, the limit of spacing is chosen between 1m to 3m, and range of the number of piles is 1 to 6. The combinations of (S, N) is as follows: (1m, 2), (1m, 3), (1m, 4), (1m, 6), (2m, 2), (2m, 3), (2m, 4), (2m, 6), (3m, 2), (3m, 3), (3m, 4), (3m, 6).

- **Step 3.** Further, for each combination of (S, N) the analysis is conducted and the relationship between the resulting reliability index and the location of a pile is plotted.

- **Step 4.** From the results depicted in Figure 6.3 and Table 6.4 it is evident that the reliability index tends to decrease with an increase in spacing (S) up to 2 m and a depth of 8 m, irrespective of the number of piles (N), and then increases slightly when the spacing (S) is increased to 3 m, with change in depth of up to 10 m. The location of 5 m provides the highest reliability index for the given spacing (S) and number (N). From these studies any alliance between (1m, 2), (1m, 3), (1m, 4) and (1m, 6) at depth 5 m are selected.

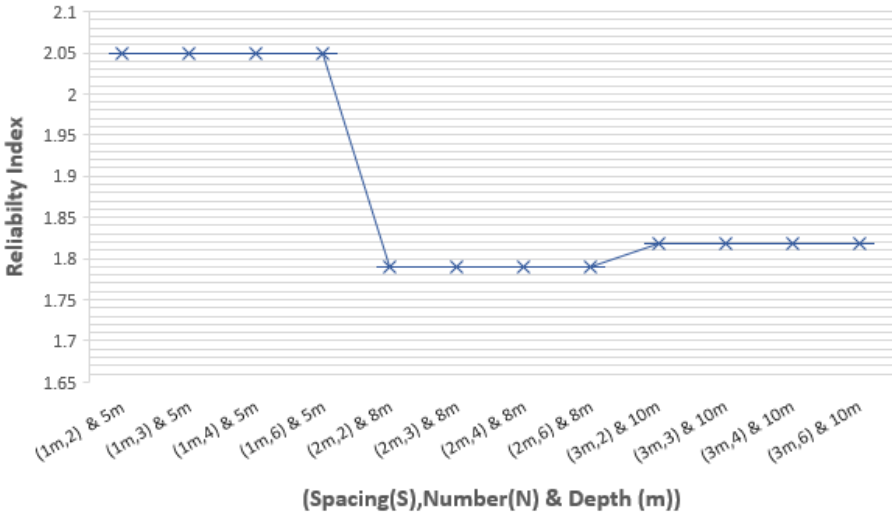

Figure 6.3: Reliability index(β) computed for (S,N) combination of piles with depth

Table 6.4: Comparison between reliability index and factor of safety of pile slope design analysis.

(Spacing S, Number N)	Reliability Index (β)	Depth (m)	Factor of Safety (mean)
(1m,2)	2.05	5	1.6225
(1m,3)	2.05	5	1.6225
(1m,4)	2.05	5	1.6225
(1m,6)	2.05	5	1.6225
(2m,2)	1.79	8	1.5661
(2m,3)	1.79	8	1.5661
(2m,4)	1.79	8	1.5661
(2m,6)	1.79	8	1.5661
(3m,2)	1.819	10	1.5427
(3m,3)	1.819	10	1.5427
(3m,4)	1.819	10	1.5427
(3m,6)	1.819	10	1.5427

- **Step 5. Case 2.** Even though the pile reinforcement enhanced the slope stability and increased the value of the reliability index (β) up to 2.05, the slope is still in the phase of failure. Therefore, an additional design procedure is adopted to make the slope stable. The top upper silty sand layer is excavated up to 3 meters, and firm clayey silt layer and soft clayey silt layer is made homogeneous to obtain a single clayey silt layer. The properties of this homogeneous layer are assumed to be the same as the firm clayey layer, i.e., undrained shear strength as 51.277 kPa and unit weight as 19 KN/m^3.

- **Step 6.** Again pile reinforcement is provided to the excavated and modified slope with a homogeneous top layer. Continuous flight auger piles are used again with similar pile dimensions and shear force, as in the case 1 analysis. Combination of 2 piles with spacing of 1 meter are implemented. Further, the analysis is conducted us-

ing the GEO-Slope software direct Monte Carlo simulation method. Figure 6.4 presents the model of redesigned slope.

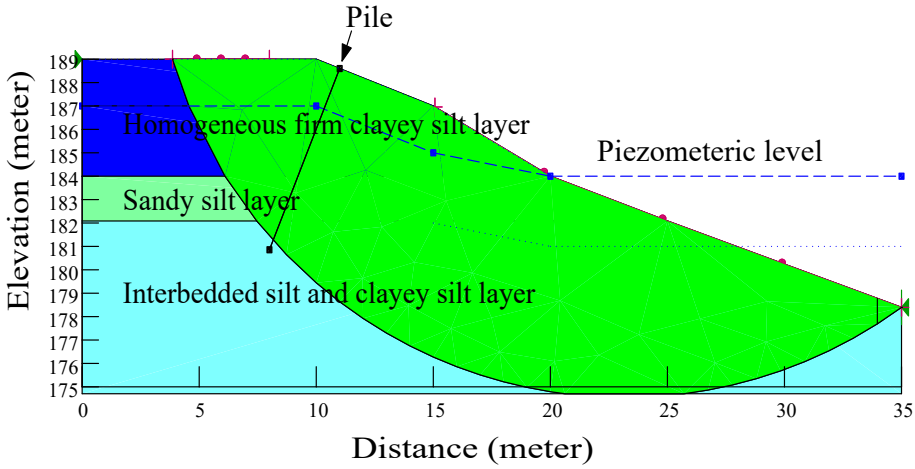

Figure 6.4: Slope model for redesigned pile slope system design

- **Step 7.** This design produces the reliability index (β) value substantially up to 3. The probability of failure value is decreased immensely, thereby resulting in the slope to be sufficiently safe. The results of the stability analysis are presented in Table 6.5. Figure 6.5 represents the probability density function of the factor of safety.

Table 6.5: Results of redesigned homogeneous layer pile slope system (Spacing-1m, Number-2 piles, and depth-5 meter)

Mean Factor of Safety	Reliability Index (β)	Probability of failure %	Factor of Safety (Max)	Factor of Safety (Min)
2.1975	2.808	0.000000	4.0724	1.1537

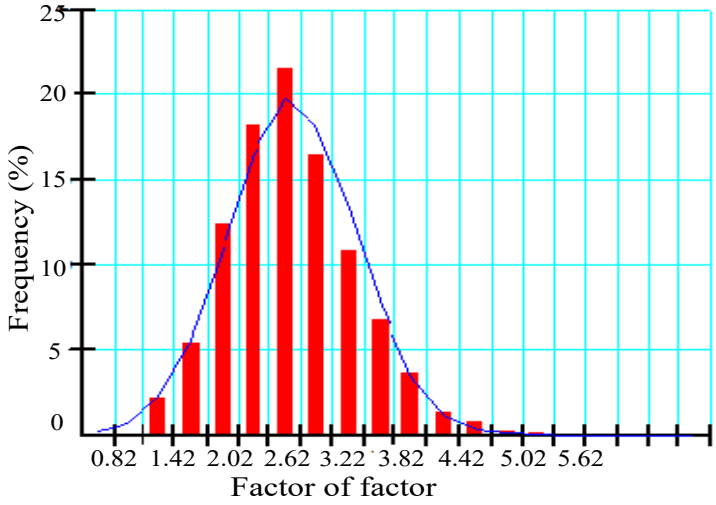

Figure 6.5: Factor of safety PDF for homogeneous layer

- **Step 8.** For reliability design optimization, the best combination of spacing (S), number (N), and depth of piles can be considered. Also analysis should include the cost comparison and construction feasibility of different types of piles. The availability of resources should also be considered and analyzed to select an optimized and economic reliability-based design of slope.

6.4 Results

The results illustrate the comparison of two cases of slope design with pile reinforcements. In the first case in (step 3), reinforcement of piles with different spacing and numbers (quantity) are provided to the exact failure slope of the on river landslide area slope analyzed in chapter 5. The results for case 1 are presented in Figure 6.3, which shows the change in reliability index(β) computed for (S,N) combination of piles at different depth. Table

6.4 depicting the comparison between reliability index and a factor of safety of pile slope. The results display that the reinforcement of piles definitely increases the reliability index of the slope from 0.452 to 2.05, but the slope is however still in the failure phase.

Further, in the second case (step 5), the slope is redesigned by excavating the first layer and making the next two layers homogeneous. Also, the different combination of pile reinforcement is employed to the slope. The results are depicted in Table 6.5. It is evident from the results that the slope is in the stable phase now with the reliability index value of 2.808 and probability of failure of almost 10^{-6}.The study in first case shows that piles reinforcement in the failure slope tends to increase the reliability index, but fails to achieve the desired probability of failure. Whereas, reinforcement of pile to the homogeneous layer slope in case 2, stabilizes the slope by decreasing the probability of failure to almost 10^{-6}. The procedure supports the importance of using a reliability-based design optimization procedure for the slope stability problem.

Precise outcomes based on the pile slope design analysis are enumerated as follows.

1. The design of a pile reinforced slope for stabilizing an unstable slope in the Nipigon River area includes the study of geotechnical variables, as well as their organization with pile reinforcement to carry out reliability analysis. The results denoted that the reliability index of an unstable slope raised handsomely after implementing the pile reinforcement.
2. The spacing, number, and length of the pile are key design variables, that can be altered in various sequences to accomplish the desired reliability index.
3. Table 6.4 gives an insight on the significance of practicing the reliability-

based design method for slope stability analysis, that a single value for factor of safety cannot be accurately determined to describe the uncertainties correlated with soil variables and the modelling uncertainties

6.5 Summary

In this chapter, a reliability-based design optimization procedure for the design of pile reinforced slope system to stabilize an unstable slope in the Nipigon River area was presented. The approach was based on a probabilistic method using maximum entropy formalism and Akaike's information criterion. Later, reliability analysis of the pile slope system was carried out by incorporating entropy generated soils variables into GEO-Slope based Monte Carlo simulation approach.

The uncertainties associated with the soil variables and the pile structural variables were characterized and systematically taken into account. The methodology illustrates the design procedure for achieving the required safe reliability index of the slope reinforced with the combination of piles depending on the spacing of piles, the number of piles and depth of the piles practiced. Finally, an additional redesigned homogeneous slope is provided with pile reinforcement to achieve reasonable probability of failure.

Chapter 7

Conclusions and Future Research

Initially, the research included soil testing on the Nipigon slope, and then it combined a comprehensive maximum entropy formalism, and Akaike's information criterion (AIC) framework for the quantification of Nipigon slope soil variables to obtain an optimal order of distribution. Furthermore, a modified entropy-based first order reliability method (FORM) slope stability analysis approach is developed in this thesis. Also, a probabilistic failure approach using the direct Monte Carlo simulation method to design the Nipigon slope.

7.1 Contributions

1. Vane shear test application on the Nipigon Slope

Foremost, the vane shear test is performed on the slope of Nipigon river area to attain the undrained shear strength values. The test outcome resulted in 123 values of undrained shear strength, which are further used in the slope stability analysis.

2. A maximum entropy formalism (MEF) and Akaike's information criterion (AIC) framework for the quantification of soil variables

The proposed approach is a distribution free method, that incorporates the inherent spatial variability of the soil properties and models explicitly the most unbiased probability density function assignment of the uncertainties

associated with soil variables. Furthermore, the method automatically improves the level of sophistication of the resulting probability distribution as per the characteristics and volume of data. This prevents us from using too many complicated models if the database is not extensive enough.

The above-described method is implemented on vane shear field test (VST) data gathered from the Nipigon slope for probabilistic distribution free quantification of shear strength parameter explicitly. The proposed approach effectively generates the third model as the most unbiased and optimal model of distribution, which is implemented in the reliability analysis and design of the Nipigon slope.

3. A new modified FORM method for entropy non-normal variables

An enhanced probabilistic approach using the modified first order reliability method (FORM) to account for entropy-generated, non-normal soil variables is adapted to provide a conceptually more rationalized way to account for uncertainties in order to carry out slope stability analysis. This approach is applicable with the aid of an explicit linear performance function created by the combined approach of GEO-Slope software and the response surface method.

The MATLAB program is developed for the modified FORM to judge the reliability of the Nipigon slope. Combined tools of GEO-Slope software and an Excel spreadsheet package for response surface method (RSM) were used to conduct a dynamic deterministic analysis. Additionally, the analysis is followed by a comparative study of the direct Monte Carlo simulation method using the GEO-Slope software to perform reliability analysis.

A combination of the MEF and modified FORM method, allowed us to estimate system failure probability of the Nipigon slope stability analysis efficiently, with probability of failure value of 40%. Also, results indicated

that modified FORM and MCS methods coincided with each other comprehensively, thereby validating the accuracy of proposed approach. Sensitivity analysis revealed that both the spatial variability and cross-correlation of the soil variables significantly affected the reliability of slope stability in spatially variable soils. Subsequently, the probability of failure rose, and the reliability index decreased with the inflation in covariance value.

4. Reliability-based design of Nipigon slope

Subsequently, a reliability-based design of failed Nipigon slope of is achieved by reinforcing slope with CFA piles. Initially, the pile reinforcement is provided to the same failure slope, ending in enhancing the reliability index, however, failed to attain stability. Conclusively, a homogeneous soil layer modification is implemented to failure slope with the pile reinforcement, that increased the stability of the slope with a probability of failure almost 10^{-6}.

7.2 Future Research

In the proposed analysis, various modified approaches are developed for geotechnical data quantification and probabilistic slope stability analysis, and the outcome of these aimed methods have depicted that they exhibit intellect in quantifying random variables and uncertainties associated with same. Additionally, the probabilistic approach appeared to be efficient in discovering the slope stability analysis. Further recommendations could include the following issues, which could be investigated to enhance the slope stability analysis procedure.

- The shear strength parameters are treated as random variables in the present study. For future research, unit weight of soil could also be

interpreted as a random variable.

- Cross-correlation between the shear strength parameters, such as cohesion and angle of friction and undrained shear strength, could be examined for stability analysis in the future.
- The water table, loading circumstances, and fluctuations in water level could also be reviewed as random variables.
- As in the present investigation, the vane shear test was conducted only up to a certain level. Additional field tests and laboratory tests could be carried out to achieve more precise soil variables values throughout the geometry of slope.
- For reliability-based design analysis, more aspects such as cost comparison, availability of resources, site access, and reinforcement material comparison based on actual engineering projects could be analyzed, while carrying out the design optimization.

Bibliography

Abbaszadeh, M., Shahriar, K., Sharifzadeh, M., & Heydari, M. (2011). Uncertainty and reliability analysis applied to slope stability: A case study from sungun copper mine. *Geotechnical and Geological Engineering*, *29*, 581-596.

Akaike, H. (1973). Information theory and an extension of the maximum likelihood principle. In B. N. P. F. Csaki (Ed.), *Second international symposium on information theory* (Vol. 2, pp. 267–281). Budapest: Akadémiai Kiado.

Allen, M., & Maute, K. (2004). Reliability-based design optimization of aeroelastic structures. *Structural and Multidisciplinary Optimization*, *27*(4), 228–242.

Babu, G. L. S., & Srivastava, A. (2010). Reliability analysis of buried flexible pipe-soil systems. *Journal of Pipeline Systems Engineering and Practice*, *1*(1), 33-41.

Baecher, G. B., & Christian, J. T. (2003). *Reliability and statistics in geotechnical engineering*. John Wiley & Sons.

Baker, R. (1990). Probability estimation and information principles. *Structural Safety*, *9*(2), 97 - 116.

Bjerrum, L. (1972). Embankments on soft ground. In *Geotechnical special publication* (Vol. 2, p. 1-54). Purdue Univ.

Chandler, R. (1988). The in-situ measurement of the undrained shear strength of clays using the field vane. *Vane shear strength testing of soils: field lab studies, STP1014, ASTM*, 13-44.

Chang, C. (1992). Discrete element method for slope stability analysis. *Journal of Geotechnical Engineering*, *118*, 1889-1905.

Chowdhury, R., Flentje, P., & Bhattacharya, G. (2009). *Geotechnical slope analysis*. Crc Press.

Close, U., & McCormick, E. (1992). Where the mountains walked. *National Geographic Magazine*, *5*(41), 445-464.

Commenges, D. (2015). Information Theory and Statistics: an overview. *ArXiv e-prints*.

Conover, W. J. (2009). Distribution-free methods in statistics. *Wiley Interdisciplinary Reviews: Computational Statistics*, *1*(2), 199-207.

Cruden, D. (1996). *Landslide types and processes, special report* (Vol. 247; Tech. Rep.). Transportation Research Board, National Academy of Sciences, 247:36-75.

Cui, J., Jiang, Q., Li, S., Feng, X., Zhang, M., & Yang, B. (2017). Estimation of the number of specimens required for acquiring reliable rock mechanical parameters in laboratory uniaxial compression tests. *Engineering Geology*, *222*, 186 - 200.

Cundall, P. A. (1971). A computer model for simulating progressive, large-scale movements in blocky rock systems. In *Proc. symp. int. rock mech.* (Vol. 2). Nancy.

Deng, J., Li, X., & Gu, G. (2004). A distribution-free method using maximum entropy and moments for estimating probability curves of rock variables. , *41*, 376-376.

Deng, J., & Pandey, M. (2000). Direct estimation of quantile functions using the maximum entropy principle. *Structural Safety*, *22*(1), 61 - 79.

Deng, J., & Pandey, M. (2008a). Cross entropy quantile function estimation from censored samples using partial probability weighted moments. *Journal of Hydrology*, *363*(1), 18 - 31.

Deng, J., & Pandey, M. (2008b). Estimation of the maximum entropy quantile function using fractional probability weighted moments. *Structural Safety*, *30*(4), 307 - 319.

Deng, J., & Pandey, M. (2009a). Derivation of sample oriented quantile function using maximum entropy and self-determined probability weighted moments. *Environmetrics*, *21*(2), 113-132.

Deng, J., & Pandey, M. (2009b). Estimation of minimum cross-entropy quantile function using fractional probability weighted moments. *Probabilistic Engineering Mechanics*, *24*(1), 43 - 50.

Deng, J., & Pandey, M. (2009c). Using partial probability weighted moments and partial maximum entropy to estimate quantiles from censored samples. *Probabilistic Engineering Mechanics*, *24*(3), 407 - 417.

Deng, J., & Pandey, M. (2010). A comparison of distribution-free entropy quantile functions using probability weighted moments from complete or censored samples. In F. Furuta & Shinozuka (Eds.), *Safety, reliability and risk of structures, infrastructures and engineering systems* (p. 1276-1283). Osaka, Japan: Taylor and Francis Group,London.

Deng, J., Pandey, M., & Gu, D. (2009). Extreme quantile estimation from censored sample using partial cross-entropy and fractional partial probability weighted moments. *Structural Safety*, *31*(1), 43 - 54.

Deng, J., Pandey, M. D., & Xie, W. C. (2012). Maximum entropy principle and partial probability weighted moments. *AIP Conference Proceedings*, *1443*(1), 190-197.

Dian Qing, L., Zhi Yong, Y., Zi Jun, C., Siu Kui, A., & Kok Kwang, P. (2017). System reliability analysis of slope stability using generalized subset simulation. *Applied Mathematical Modelling*, *46*, 650 - 664.

Dodds, R. B., Burak, J. P., & Eigenbrod, K. D. (1993). Nipigon river landslide. *International Conference on Case Histories in Geotechnical Engineering*, *20*, 517-523.

Draper, N. R. (1992). *Introduction to box and wilson (1951) on the experimental attainment of optimum conditions* (S. Kotz & N. L. Johnson, Eds.). New York, NY: Springer New York.

Enevoldsen, I. (1994). Reliability-based optimization as an information tool. *Journal of Structural Mechanics*, *22*, 117-135.

Enevoldsen, I., & Sørensen., J. D. (1994). Reliability-based optimization in structural engineering. *Structural Safety*, *15*(3), 169 - 196.

Fredlund, G., & Krahn, J. (2011). Comparison of slope stability methods. *Canadian Geotechnical Journal*, *14*, 429-439.

Griffiths, D. V., & Lane, P. A. (1999). Slope stability analysis by finite elements. *Géotechnique*, *49*(3), 387-403.

Haldar, A., & Mahadevan, S. (2000). *Probability, reliability, and statistical methods in engineering design*. New York: John Wiley and Sons.

Harr, M. E. (1987). *Reliability-based design in civil engineering*. New York: McGraw-Hill.

Hassiotis, S., Chameau, J. L., & Gunaratne, M. (1997). Design method for stabilization of slopes with piles. *Journal of Geotechnical and Geoenvironmental Engineering*, *123*(4), 314-323.

Hong, S. (2012). *Non-deterministic analysis of slope stability based on numerical simulation* (Unpublished master's thesis). By the Faculty of

Geosciences, Geoengineering and Mining of the Technische Universität Bergakademie Freiberg, Geoengineering and Mining of the Technische Universität Bergakademie Freiberg.

Huang, Y. H. (2014). *Slope stability analysis by the limit equilibrium method : fundamentals and methods*. Reston, Virginia : ASCE Press.

Hutchinson, S., & Bandalos, D. (1997). Guide to monte carlo simulation research for applied researchers. *Journal of Vocational Education Research*, *22*(4), 233-245.

ISSMGE. (2004). *Technical Committee on Risk Assessment and Management Glossary of Risk Assessment Terms* (Tech. Rep.). ISSMGE TC32.

Janbu, N. (1973). Slope stability computations. , *Casagrande Volume*, 47-86.

Jay, A., Nagaratnam, S., & Braja, D. (2016). *Correlations of soil and rock properties in geotechnical engineering*. New Delhi: Springer.

Kang, K., Zerkal, O. V., Liu, J., Huang, S., & Tao, D. (2018). Comparison of russian, chinese and european seismic design on pseudo-static seismic coefficient in slope analysis. *Journal of Civil Engineering and Construction*, *7*(2), 57–62.

Kao, J. (1985). Application of pile retaining wall to building protection and slope stabilization. In *Theory and practice in foundation engineering* (p. 209-215). 38th Canadaian Geotechnical Conference.

Kellet, J. (2014). *Disaster risk reduction makes development sustainable.* UN Development Programme.

Kenneth, L. I., Graeme, I. O., & Wee, W. (1983). *Geotechnical engineering*. Boston ; Melbourne : Pitman.

Kullback, S., & Leibler, R. A. (1951). On information and sufficiency. *The Annals of Mathematical Statistics*, *22*(1), 79–86.

Li, C., Wang, W., & Wang, S. (2012). Maximum-entropy method for evaluating the slope stability of earth dams. *Entropy*, *14*(10), 1864–1876.

Li, J., & Xu, G. (2011). Seismic reliability analysis of hydraulic aqueduct with maximum entropy method. In *Advanced research on material engineering, chemistry, bioinformatics* (Vol. 282, pp. 120–123). Trans Tech Publications.

Li, L., & Liang, R. Y. (2013). Reliability-based design for slopes reinforced with a row of drilled shafts. *International Journal for Numerical and Analytical Methods in Geomechanics*, *38*(2), 202-220.

Liang, L., Yu, W., & Zijun, C. (2014). Probabilistic slope stability analysis by risk aggregation. *Engineering Geology*, *176*, 57 - 65.

Lindley, D. V. (1956). On a measure of the information provided by an experiment. *Ann. Math. Statist.*, *27*(4), 986–1005.

Lindley, D. V. (1959). Information theory and statistics. *Journal of the American Statistical Association*, *54*(288), 825-827.

Lunne, T., & Robertson, P. K. (1997). *Cone penetration testing in geotechnical practice*. London: Blackie Academic and Professional.

Matsui, T., & San, K. (1992). Finite element slope stability analysis by shear strength reduction technique. *Soils and Foundations*, *32*(1), 59-70.

Melentijevic, S., Serrano, A., Olalla, C., & Gao, R. (2017). Incorporation of non-associative flow rules into rock slope stability analysis. *International Journal of Rock Mechanics and Mining Sciences*, *96*, 47 - 57.

Morgenstern, N. R. (1995). *Managing risk in geotechnical engineering: The third casagrande lecture* (Vol. 4). Proceedings of the 10th Pan-American Conference on soil Mechanics and Foundation Engineering, Mexico.

Morris, P. H., & Williams, D. J. (1996). Exponential longitudinal profiles of streams. *Earth Surface Processes and Landforms*, *22*(2), 143-163.

Nemcok, A., Pasek, J., & Rybar, J. (1972). Classification of landslides and other mass movements. *Rock mechanics*, *4*(2), 71–78.

Phoon, K. K., & Kulhawy, F. H. (1999). Characterization of geotechnical variability. *Canadian Geotechnical Journal*, *36*(4), 612-624.

Poulos, H. G. (1995). Design of reinforcing piles to increase slope stability. *Canadian Geotechnical Journal*, *32*(5), 808-818.

Priceputu, A. (2013). Comparison between stochastic and deterministic approaches in slope stability analyis. In *Science and technologies in geology, exploration and minning.* 13th International Multidisciplinary Scientific Geoconference Sgem.

Rosenblueth, E. (1981). Two-point estimates in probabilities. *Applied Mathematical Modelling*, *5*(5), 329 - 335.

Rosenkrantz, R. D., & Baierlein, R. (1984). E. t. jaynes: Papers on probability, statistics and statistical physics. *American Journal of Physics*, *52*(2), 190-191.

Salgado, R. (2006). *The engineering of foundations*. McGraw-Hill Education.

Santamarina, J. C., Altschaeffl, A. G., & Chameau, J. L. (1992). Reliability of slopes: Incorporating qualitative information (abridgment). *Transportation Research Board*, 1-5.

Shen, H. (1984). *Non-deterministic analysis of slope stability based on numerical simulation* (Unpublished master's thesis). By the Faculty of Geosciences, Geoengineering and Mining of the Technische Universität Bergakademie Freiberg, Freiberg.

Shien, N. K. (2005). *Reliability analysis on the stability of slopes* (masters thesis). University technology Malaysia, Malaysia.

Shin, E. C., Patra, C. R., & Rout, A. K. (2006). Automated stability analysis of slopes stabilized with piles. *KSCE Journal of Civil Engineering*, *10*(5), 333–338.

Sobczyk, K. (2003). Reconstruction of random material microstructures: Patterns of maximum entropy. *Probabilistic Engineering Mechanics*, *18*, 279-287.

Sobczyk, K., & Trcebicki, J. (1999). Approximate probability distributions for stochastic systems: maximum entropy method. *Computer Methods in Applied Mechanics and Engineering*, *168*(1), 91 - 111.

Subramaniam, P. (2011). *Reliability based analysis of slope, foundation and retaining wall using finite element method* (Unpublished master's thesis). Department of civil engineering NIT, Rourkela, India.

Survey, U. G. (2000). *Landslide hazards* (Tech. Rep. No. 071-00). Reston, VA USGS Publications Warehouse: Author.

Swan, C. C., & Kyo, S. Y. (1999). Limit state analysis of earthen slopes using dual continuum/fem approaches. *International Journal for Numerical and Analytical Methods in Geomechanics*, *23*(12), 1359-1371.

Tobutt, D. C. (1982). Monte carlo simulation methods for slope stability. *Computers and Geosciences*, *8*(2), 199 - 208.

Tu, J., Choi, K., & Park, Y. (1999). A new study on reliability-based design optimization. *Journal of Mechanical Design*, *121*(4), 557–564.

Walker, B. F. (1983). Vane shear strength testing. In M. Ervin (Ed.), *In situ testing for geotechnical investigations* (p. 65–72). Rotterdam: A A Balkema.

Wang, L., Hwang, J. H., Juang, C. H., & Atamturktur, S. (2013). Reliability-based design of rock slopes — a new perspective on design robustness. *Engineering Geology*, *154*, 56 - 63.

Whitlow, R. (2000). *Basic soil mechanics* (Vol. 4). Pearson.

Wolff, T. (1985). *Analysis and design of embankment dam slopes : a probabilistic approach* (PhD thesis). Purdue University, USA.

Wolff, T. (1994). *Evaluating the reliability of existing levees* (Tech. Rep.). US Army Engineer Waterways Experiment Station.

Wolff, T. (1996). Probabilistic slope stability in theory and practice. , 419-433.

Zhang, J., & Gu, C. (2015). Maximum entropy method for operational loads feedback using concrete dam displacement. *Entropy*, *17*(5), 2958–2972.

Zhang, S. (1990). *Evaluation and updating of slope reliability (with particular reference to optimization and probabilistic analysis)* (Unpublished master's thesis). Department of civil and mining engineering university of wollongong, New South Wales, Australia.

Zhao, Y., & Frey, H. C. (2004). Quantification of variability and uncertainty for censored data sets and application to air toxic emission factors. *Risk Analysis*, *24*(4), 1019-1034.

Appendix

Appendix A

Table 7.1: The design of experiments values

dFF2				
0	0	0	0	0
0	0	0	0	1
0	0	0	1	0
0	0	0	1	1
0	0	1	0	0
0	0	1	0	1
0	0	1	1	0
0	0	1	1	1
0	1	0	0	0
0	1	0	0	1
0	1	0	1	0
0	1	0	1	1
0	1	1	0	0
0	1	1	0	1
0	1	1	1	0
0	1	1	1	1
1	0	0	0	0
1	0	0	0	1
1	0	0	1	0
1	0	0	1	1
1	0	1	0	0
1	0	1	0	1
1	0	1	1	0
1	0	1	1	1
1	1	0	0	0
1	1	0	0	1
1	1	0	1	0
1	1	0	1	1
1	1	1	0	0
1	1	1	0	1
1	1	1	1	0
1	1	1	1	1

Table 7.2: FOS obtained from RSM analysis on Nipigon slope parameters using Geo-Slope 2007

	Layer 1	Layer 2	Layer 3	Layer 4	Layer 5	FOS
(0) = $\mu + 1.65\sigma$	44.85	76.66	37.38	44.85	44.85	
(1) = $\mu - 1.65\sigma$	15.15	25.89	12.63	15.15	15.5	
1	44.85	76.66	37.38	44.85	44.85	1.896
2	44.85	76.66	37.38	44.85	15.5	1.232
3	44.85	76.66	37.38	15.15	44.85	1.793
4	44.85	76.66	37.38	15.15	15.5	1.106
5	44.85	76.66	37.38	44.85	44.85	1.896
6	44.85	76.66	37.38	44.85	15.5	1.232
7	44.85	76.66	37.38	15.15	44.85	1.793
8	44.85	76.66	37.38	15.15	15.5	1.106
9	44.85	25.89	37.38	44.85	44.85	1.751
10	44.85	25.89	37.38	44.85	15.5	0.811
11	44.85	25.89	37.38	15.15	44.85	1.119
12	44.85	25.89	37.38	15.15	15.5	0.748
13	44.85	25.89	12.63	44.85	44.85	1.033
14	44.85	25.89	12.63	44.85	15.5	0.701
15	44.85	25.89	12.63	15.15	44.85	0.759
16	44.85	25.89	12.63	15.15	15.5	0.646
17	15.15	76.66	37.38	44.85	44.85	1.886
18	15.15	76.66	37.38	44.85	15.5	1.214
19	15.15	76.66	37.38	15.15	44.85	1.784
20	15.15	76.66	37.38	15.15	15.5	1.091
21	15.15	76.66	12.63	44.85	44.85	1.614
22	15.15	76.66	12.63	44.85	15.5	1.053
23	15.15	76.66	12.63	15.15	44.85	1.333
24	15.15	76.66	12.63	15.15	15.5	0.939
25	15.15	25.89	37.38	44.85	44.85	1.727
26	15.15	25.89	37.38	44.85	15.5	0.807
27	15.15	25.89	37.38	15.15	44.85	1.107
28	15.15	25.89	37.38	15.15	15.5	0.745
29	15.15	25.89	12.63	44.85	44.85	0.983
30	15.15	25.89	12.63	44.85	15.5	0.698
31	15.15	25.89	12.63	15.15	44.85	0.755
32	15.15	25.89	12.63	15.15	15.5	0.643

Response Surface Method to develop implicit function using Excel-sheet solver in Figure rsmsol and Figure 7.2:

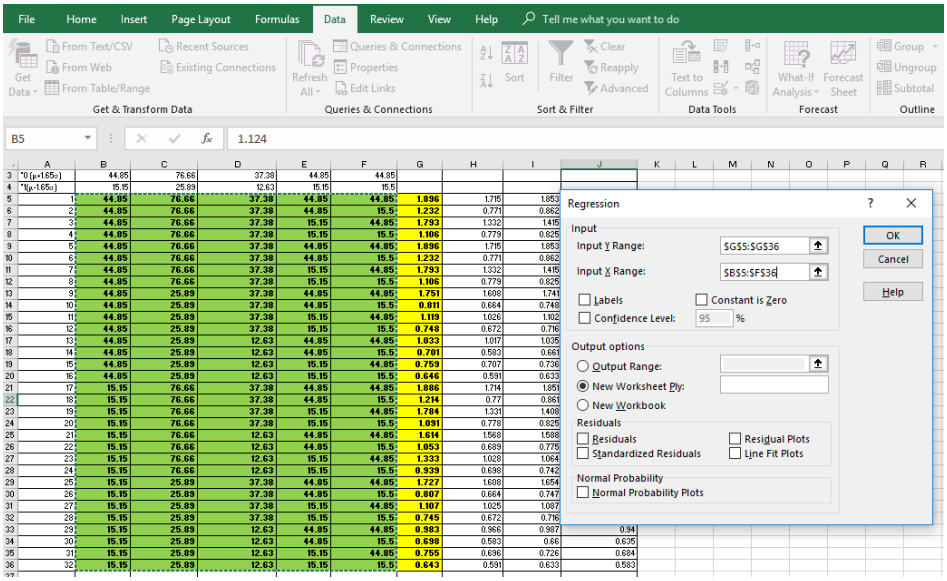

Figure 7.1: Excel solver for regression analysis

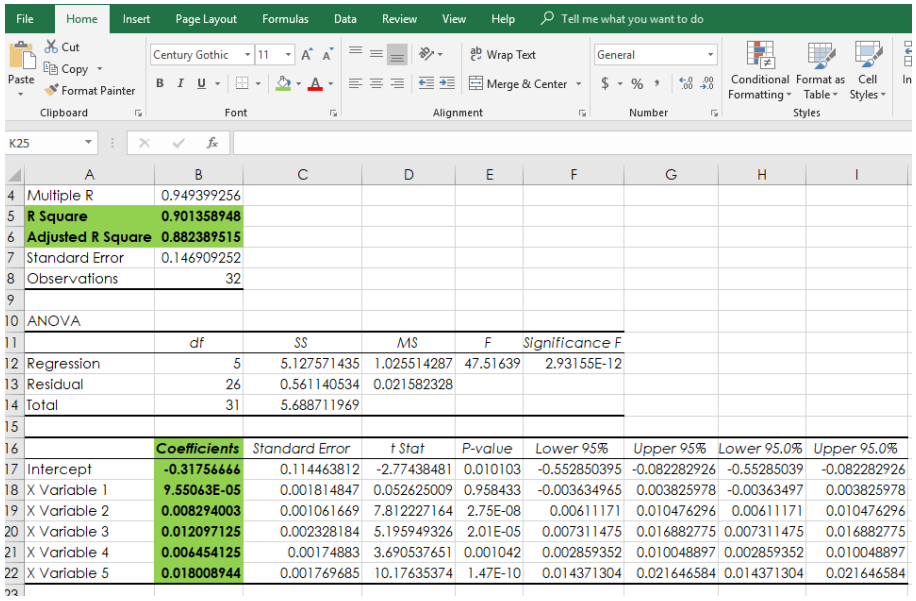

	A	B	C	D	E	F	G	H	I
4	Multiple R	0.949399256							
5	**R Square**	**0.901358948**							
6	**Adjusted R Square**	**0.882389515**							
7	Standard Error	0.146909252							
8	Observations	32							
9									
10	ANOVA								
11		*df*	*SS*	*MS*	*F*	*Significance F*			
12	Regression	5	5.127571435	1.025514287	47.51639	2.93155E-12			
13	Residual	26	0.561140534	0.021582328					
14	Total	31	5.688711969						
15									
16		***Coefficients***	*Standard Error*	*t Stat*	*P-value*	*Lower 95%*	*Upper 95%*	*Lower 95.0%*	*Upper 95.0%*
17	Intercept	**-0.31756666**	0.114463812	-2.77438481	0.010103	-0.552850395	-0.082282926	-0.55285039	-0.082282926
18	X Variable 1	**9.55063E-05**	0.001814847	0.052625009	0.958433	-0.003634965	0.003825978	-0.00363497	0.003825978
19	X Variable 2	**0.008294003**	0.001061669	7.812227164	2.75E-08	0.00611171	0.010476296	0.00611171	0.010476296
20	X Variable 3	**0.012097125**	0.002328184	5.195949326	2.01E-05	0.007311475	0.016882775	0.007311475	0.016882775
21	X Variable 4	**0.006454125**	0.00174883	3.690537651	0.001042	0.002859352	0.010048897	0.002859352	0.010048897
22	X Variable 5	**0.018008944**	0.001769685	10.17635374	1.47E-10	0.014371304	0.021646584	0.014371304	0.021646584

Figure 7.2: Coefficients of variables to develop a response surface model performance function

Appendix B

Table 7.3: Data of 48-OP basalt rock uniaxial compressive strength

No.	Uniaxial compressive strength (Mpa)	No.	Uniaxial compressive strength (Mpa)
1	61.2	25	129.6
2	63.2	26	131.8
3	66.6	27	136.4
4	86.5	28	137.4
5	90.8	29	139
6	97.7	30	140
7	98	31	140.7
8	99.7	32	142.2
9	102.4	33	142.6
10	104.3	34	144.4
11	106.4	35	147.5
12	109.7	36	148.9
13	112	37	150.9
14	112	38	152.5
15	114.6	39	152.9
16	114.9	40	159.1
17	115	41	162.6
18	118.7	42	165.3
19	119.7	43	165.5
20	123.2	44	167.9
21	125.8	45	174.7
22	128.9	46	177.2
23	129.2	47	191.7
24	129.6	48	191.9

Table 7.4: Data of 220 sample values of warehouse live load lb/ft^2

0.0	7.8	36.2	60.6	64.0	64.2	79.2	88.4	38.0	72.7
72.2	72.6	74.4	21.8	17.1	48.5	16.8	105.9	57.2	75.7
225.7	42.5	59.8	41.7	39.9	55.5	67.2	122.8	45.2	62.9
55.1	55.9	87.7	59.2	63.1	58.8	67.7	90.4	43.3	55.2
36.6	26.0	90.5	23.0	43.5	52.1	102.1	71.7	4.1	37.3
129.4	66.4	138.7	127.9	90.9	46.9	197.5	151.1	157.3	197.0
134.6	73.4	80.9	53.3	80.1	62.9	150.8	102.2	6.4	45.4
121.0	106.2	94.4	139.6	152.5	70.2	111.8	174.1	85.4	83.0
178.8	30.2	44.1	157.0	105.3	87.0	50.1	198.0	86.7	64.6
78.6	37.0	70.7	83.0	179.7	180.2	60.6	212.4	72.2	86.0
94.5	24.1	87.3	80.6	74.8	72.4	131.1	116.1	53.6	99.1
40.2	23.4	8.4	42.6	43.4	27.4	63.8	18.4	16.2	58.7
92.2	49.8	50.9	116.4	122.9	132.3	105.2	160.3	28.7	46.8
99.5	106.9	55.9	136.8	110.4	123.5	92.4	160.9	45.4	96.3
88.5	48.4	62.3	71.3	133.2	92.1	111.7	67.9	53.1	39.7
93.2	55.0	80.8	143.5	122.3	184.2	150.0	57.6	6.8	53.3
96.1	54.8	63.0	228.3	139.3	59.1	112.1	50.9	158.6	139.1
213.7	65.7	90.3	198.4	97.5	155.1	163.4	155.3	229.5	75.0
137.6	62.5	156.5	154.1	134.3	81.6	194.4	155.1	89.3	73.4
79.8	68.7	85.6	141.6	100.7	106.0	131.1	157.4	80.2	65.0
78.5	118.2	126.4	33.8	124.6	78.9	146.0	100.3	97.8	75.3
24.8	55.6	135.6	56.3	66.9	72.2	105.4	98.9	101.7	58.2